PHYSICAL REVIEW D **82,** 023520 (2010)

General CMB and primordial trispectrum estimation

D. M. Regan, E. P. S. Shellard, and J. R. Fergusson

Centre for Theoretical Cosmology, Department of Applied Mathematics and Theoretical Physics, University of Cambridge, Wilberforce Road, Cambridge CB3 0WA, United Kingdom

(Received 12 May 2010; published 23 July 2010)

In this paper we present trispectrum estimation methods which can be applied to general nonseparable primordial and CMB trispectra. We review the relationship between the reduced CMB trispectrum and the reduced primordial trispectrum. We present a general optimal estimator for the connected part of the trispectrum, for which we derive a quadratic term to incorporate the effects of inhomogeneous noise and masking. We describe a general algorithm for creating simulated maps with given arbitrary (and independent) power spectra, bispectra, and trispectra. We propose a universal definition of the trispectrum parameter T_{NL}, so that the integrated trispectrum on the observational domain can be consistently compared between theoretical models. We define a shape function for the primordial trispectrum, together with a shape correlator and a useful parametrization for visualizing the trispectrum; these methods might also be applied to the late-time trispectrum for large-scale structure. We derive separable analytic CMB solutions in the large-angle limit for constant and local models. We present separable mode decompositions which can be used to describe any primordial or CMB trispectra on their respective wave number or multipole domains. By extracting coefficients of these separable basis functions from an observational map, we are able to present an efficient estimator for any given theoretical model with a nonseparable trispectrum. The estimator has two manifestations, comparing the theoretical and observed coefficients at either primordial or late times, thus encompassing a wider range of models, such as secondary anisotropies, lensing, and cosmic strings. We show that these mode decomposition methods are numerically tractable with order l^5 operations for the CMB estimator and approximately order l^6 for the general primordial estimator (reducing to order l^3 in both cases for a special class of models). We also demonstrate how the trispectrum can be reconstructed from observational maps using these methods.

DOI: 10.1103/PhysRevD.82.023520 PACS numbers: 98.80.Cq, 98.80.Es

I. INTRODUCTION

Single-field slow-roll inflationary fluctuations in the standard picture of cosmology predict a nearly scale-invariant spectrum of adiabatic perturbations with a nearly Gaussian distribution. Hence it can be described very accurately by its angular power spectrum. These predictions agree well with measurements of the CMB and large-scale structure, such as those provided by the Wilkinson Microwave Anisotropy Probe (WMAP) satellite and the Sloan Digital Sky Survey. However, it remains possible that there exists a mechanism for generating large non-Gaussianities in the early Universe. Measurements of such non-Gaussianities open up the opportunity of investigating the physics of the early Universe, including different inflationary models and competing alternative scenarios. In order to study such observations, higher order correlators, beyond the two-point function, offer possibly the best prospects. General methods for comparing the three-point correlator, dubbed the bispectrum, were developed in [1–3]. In those papers an integrated measure of the bispectrum was defined, as well as a set of formalisms for comparing, evolving, and constraining the bispectrum in the case of both the primordial and CMB three-point correlators. In this paper we will generalize many of these methods to the four-point correlator which is denoted as the trispectrum. We will emphasize the application of these methods to the primordial and CMB trispectra. The primary motivation for this paper is to develop formalisms to bring observations to bear on this broader class of cosmological models. We will demonstrate that despite the complexity of trispectrum estimation, these methods are numerically tractable given present resources, even at Planck satellite resolution.

In order to get large non-Gaussianities we must move away from the standard single-field slow-roll inflation [4]. Multifield inflation allows the possibility for superhorizon evolution. Non-Gaussianities are generated when this evolution is nonlinear. We can consider superhorizon behavior as occurring in patches separated by horizons which evolve independently of each other. This locality in position space translates to nonlocality in momentum space and indicates that, for such models, we expect the signal to peak for $k_4 \ll k_1, k_2, k_3$. This forms the so-called local model. Such models have been investigated in the context of the trispectrum in [5–13]. Since subhorizon modes oscillate and so average out, the only chance to have large non-Gaussianities in single-field inflationary models is when all modes have similar wavelengths and exit at the same time. A nonstandard kinetic term allows for such a possibility. Since the signal peaks when the modes have similar

wavelengths, these forms are known as equilateral models and have been investigated using the trispectrum in [14–20]. It should be noted that this amplification of nonlinear effects around the time the modes exit the horizon is not possible for slow-roll single-field inflation. It has also been shown in [21,22] that a large trispectrum may be generated in the ghost inflation model. These models are so-called as they are based on the idea of a ghost condensate, i.e. a kind of fluid with equation of state $p = -\rho$, that can fill the Universe, and which provides an alternative method of realizing de Sitter phases in the early Universe. Of course, there are other methods that can generate non-Gaussianity, such as having sharp features in the potential or a non-Bunch-Davies vacuum. Also, there are models which have features that resemble the aforementioned forms in different regimes, e.g. quasisingle field inflation [23], or have mixed contributions, e.g. in multifield Dirac-Born-Infeld inflation [24].

One of the motivations for studying the four-point correlator is that it may be possible that the bispectrum is suppressed while the trispectrum is still large. In particular, this behavior may be realized in quasisingle field inflation [23] or in the curvaton model [25]. It also occurs in the case of cosmic strings where the bispectrum is suppressed by symmetry considerations [26,27]. The effects of non-Gaussianity could also be detectable in a wide range of astrophysical measurements, such as cluster abundances and the large-scale clustering of highly biased tracers. In [28] the possibility of using the galaxy bispectrum to constrain the local form of the trispectrum has been reviewed.

The trispectrum $T(k_1, k_2, k_3, k_4)$ is generally parametrized using the variable τ_{NL}, which schematically is given by the ratio $\tau_{NL} \approx T(k, k, k, k)/P(k)^3$. Standard slow-roll inflation predicts $\tau_{NL} \lesssim r/50$, where $r < 1$ is the tensor to scalar ratio [11]. Such a low signal would be undetectable since it is below the level of non-Gaussian contamination that would be expected from secondary anisotropies, $\tau_{NL} \approx \mathcal{O}(1)$. Using the analysis of N-point probability distribution of the CMB anisotropies [29], where a local nonlinear perturbative model $\Phi = \Phi_L + f_{NL}(\Phi_L^2 - \langle\Phi_L^2\rangle) + g_{NL}\Phi_L^3 + \mathcal{O}(\Phi_L^4)$ is used to characterize the large-scale anisotropies, the constraint $-5.6 \times 10^5 < g_{NL} < 6.4 \times 10^5$ was obtained.[1] For the more general case, there is only a weak experimental bound imposed on non-Gaussianity by the trispectrum, which is roughly $|\tau_{NL}| \lesssim 10^8$ [30]. In [31,32] an improved constraint on τ_{NL} was presented using estimators to allow a joint fit of f_{NL} and g_{NL} using the trispectrum of 5-yr Wilkinson Microwave Anisotropy Probe data. However, the analysis therein included an incomplete formula for the CMB trispectrum due to local non-Gaussianity.[2] Nonetheless, the approach indicates that vast improvements to trispectrum constraints should be achievable in the near future. In fact, it is expected that the Planck satellite will be sensitive to a value of $|\tau_{NL}| \sim 560$ [33].

The analysis of the trispectrum is a computationally intensive operation. In fact, only the trispectrum induced by the local shape has been constrained so far by CMB data. The local form is an example of a separable shape—a notion which we will define more concretely in this paper. Essentially, since the primordial trispectrum is a six-dimensional quantity, separability means the trispectrum is the product of one-dimensional functions of each of these variables. Exploiting this separability reduces the problem from one of $\mathcal{O}(l_{\max}^7)$ operations to a more manageable $\mathcal{O}(l_{\max}^5)$. In special cases we get a further reduction to $\mathcal{O}(l_{\max}^3)$.

In the next section we shall describe the CMB trispectrum and its relation to the primordial equivalent. We will make use of a particular parametrization of the reduced primordial trispectrum and exploit a Legendre series expansion in terms of one of these parameters to write an expression for the reduced CMB trispectrum which is valid in general. We will also outline a general correlation method for comparing different trispectra. In this section we will also give a formula for the kurtosis in terms of the multipoles. In Sec. III we define a shape function which is a scale-invariant form of the trispectrum. Using this function we define a shape correlator that is expected to predict closely the correlation between the respective trispectra. Next, we show how to decompose this shape in order to provide a method for visualizing trispectra. We apply this visualization to the case of the local and equilateral models which we describe in Sec. IV. We also present the Sachs-Wolfe limit ($l < 100$) for the local and constant models. In Sec. V we describe how to form a mode expansion for general nonseparable shapes. This provides a rigorous method to find a separable approximation to any shape and therefore makes analysis of the trispectrum far more tractable. This expansion can be performed for both the primordial and CMB trispectra. Of immediate relevance in terms of the Planck satellite is to find a general measure for the size of the trispectrum. This is addressed in Sec. VI in both the primordial and CMB cases. It is clearly desirable to be able to reconstruct the underlying trispectrum given the data. As we shall describe in Sec. VII, this is a computationally intensive task, but it is tractable. We will observe here that there is a degeneracy in reconstruction of the primordial trispectrum, implying that only the zeroth Legendre mode is recoverable. Finally, in Sec. VIII we outline a method for performing CMB map simulations for given general bispectra and trispectra.

[1] It should be noted that for single-field local inflation $\tau_{NL}^{\rm loc} = (\frac{5}{6}f_{NL})^2$. Since f_{NL} is constrained by the bispectrum, g_{NL} is the quantity that is constrained by the trispectrum directly in this case.

[2] The formula for the reduced local CMB trispectrum has been used in place of the full local CMB trispectrum, which appears to simplify the analysis.

II. THE CMB TRISPECTRUM

A. Definition of the primordial and CMB trispectra

We are concerned with the analysis of the four-point function induced by a non-Gaussian primordial gravitational potential $\Phi(\mathbf{k})$ in the CMB temperature fluctuation field. The temperature anisotropies may be represented using the a_{lm} coefficients of a spherical harmonic decomposition of the cosmic microwave sky,

$$\frac{\Delta T}{T}(\hat{\mathbf{n}}) = \sum_{l,m} a_{lm} Y_{lm}(\hat{\mathbf{n}}). \tag{1}$$

The primordial potential Φ induces the multipoles a_{lm} via a convolution with the transfer functions $\Delta_l(k)$ through the relation

$$a_{lm} = 4\pi(-i)^l \int \frac{d^3k}{(2\pi)^3} \Delta_l(k) \Phi(\mathbf{k}) Y_{lm}(\hat{\mathbf{k}}). \tag{2}$$

The connected part of the four-point correlator of the a_{lm} gives us the trispectrum. In particular,

$$\begin{aligned} T_{l_1m_1l_2m_2l_3m_3l_4m_4} &= \langle a_{l_1m_1} a_{l_2m_2} a_{l_3m_3} a_{l_4m_4} \rangle_c \\ &= (4\pi)^4 (-i)^{\sum_i l_i} \int \frac{d^3k_1 d^3k_2 d^3k_3 d^3k_4}{(2\pi)^{12}} \Delta_{l_1}(k_1) \Delta_{l_2}(k_2) \Delta_{l_3}(k_3) \Delta_{l_4}(k_4) \langle \Phi(\mathbf{k_1}) \Phi(\mathbf{k_2}) \Phi(\mathbf{k_3}) \Phi(\mathbf{k_4}) \rangle_c \\ &\quad \times Y_{l_1m_1}(\hat{\mathbf{k}}_\mathbf{1}) Y_{l_2m_2}(\hat{\mathbf{k}}_\mathbf{2}) Y_{l_3m_3}(\hat{\mathbf{k}}_\mathbf{3}) Y_{l_4m_4}(\hat{\mathbf{k}}_\mathbf{4}), \end{aligned} \tag{3}$$

where $k_i = |\mathbf{k}_i|$ and the subscript c is used to denote the connected component. Naively, we would define the primordial trispectrum as

$$\langle \Phi(\mathbf{k_1}) \Phi(\mathbf{k_2}) \Phi(\mathbf{k_3}) \Phi(\mathbf{k_4}) \rangle_c = (2\pi)^3 \delta(\mathbf{k_1} + \mathbf{k_2} + \mathbf{k_3} + \mathbf{k_4}) T'_\Phi(\mathbf{k}_1, \mathbf{k}_2, \mathbf{k}_3, \mathbf{k}_4).$$

Here, the four wave vectors form a quadrilateral as shown in Fig. 1.

However, a more useful definition is to write

$$\langle \Phi(\mathbf{k_1}) \Phi(\mathbf{k_2}) \Phi(\mathbf{k_3}) \Phi(\mathbf{k_4}) \rangle_c = (2\pi)^3 \int d^3K \delta(\mathbf{k_1} + \mathbf{k_2} + \mathbf{K}) \delta(\mathbf{k_3} + \mathbf{k_4} - \mathbf{K}) T_\Phi(\mathbf{k_1}, \mathbf{k_2}, \mathbf{k_3}, \mathbf{k_4}; \mathbf{K}). \tag{4}$$

Here the delta function indicates that the diagonal $\mathbf{K}$ makes triangles with $(\mathbf{k_1}, \mathbf{k_2})$ and $(\mathbf{k_3}, \mathbf{k_4})$, respectively. Of course there are symmetries implicit in this definition of T_Φ—namely, that we may form triangles with different combinations of the vectors. In particular,

$$\begin{aligned} T_\Phi(\mathbf{k}_1, \mathbf{k}_2, \mathbf{k}_3, \mathbf{k}_4; \mathbf{K}) &= P_\Phi(\mathbf{k}_1, \mathbf{k}_2, \mathbf{k}_3, \mathbf{k}_4; \mathbf{K}) + \int d^3K' [\delta(\mathbf{k_3} - \mathbf{k_2} - \mathbf{K} + \mathbf{K}') P_\Phi(\mathbf{k}_1, \mathbf{k}_3, \mathbf{k}_2, \mathbf{k}_4; \mathbf{K}') \\ &\quad + \delta(\mathbf{k_4} - \mathbf{k_2} - \mathbf{K} + \mathbf{K}') P_\Phi(\mathbf{k}_1, \mathbf{k}_4, \mathbf{k}_3, \mathbf{k}_2; \mathbf{K}')], \end{aligned} \tag{5}$$

where P_Φ are constructed using a reduced trispectrum $\mathcal{T}_\Phi$ via

$$\begin{aligned} P_\Phi(\mathbf{k}_1, \mathbf{k}_2, \mathbf{k}_3, \mathbf{k}_4; \mathbf{K}) &= \mathcal{T}_\Phi(\mathbf{k}_1, \mathbf{k}_2, \mathbf{k}_3, \mathbf{k}_4; \mathbf{K}) + \mathcal{T}_\Phi(\mathbf{k}_2, \mathbf{k}_1, \mathbf{k}_3, \mathbf{k}_4; \mathbf{K}) + \mathcal{T}_\Phi(\mathbf{k}_1, \mathbf{k}_2, \mathbf{k}_4, \mathbf{k}_3; \mathbf{K}) \\ &\quad + \mathcal{T}_\Phi(\mathbf{k}_2, \mathbf{k}_1, \mathbf{k}_4, \mathbf{k}_3; \mathbf{K}). \end{aligned} \tag{6}$$

Therefore, we need only consider the reduced trispectrum $\mathcal{T}$ from one particular arrangement of the vectors and form the other contributions by permuting the symbols.

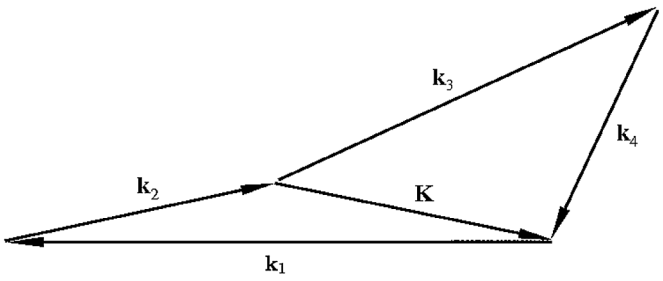

FIG. 1. Quadrilateral defined by the four wave vectors $\mathbf{k}_i$. The diagonal is represented for $\mathbf{K}$.

The CMB trispectrum may also be written in a rotationally invariant way as

$$\begin{aligned} T_{l_1m_1l_2m_2l_3m_3l_4m_4} &= \sum_{LM} (-1)^M \begin{pmatrix} l_1 & l_2 & L \\ m_1 & m_2 & -M \end{pmatrix} \\ &\quad \times \begin{pmatrix} l_3 & l_4 & L \\ m_3 & m_4 & M \end{pmatrix} T^{l_1l_2}_{l_3l_4}(L). \end{aligned} \tag{7}$$

The Wigner $3j$ symbols impose the triangle conditions on the multipole combinations (l_1, l_2, L) and (l_3, l_4, L). As in the case of the primordial trispectrum, there are implicit symmetries in this definition. In a similar manner to the primordial case we can write

$$T_{l_1m_1l_2m_2l_3m_3l_4m_4} = \sum_{LM}(-1)^M \begin{pmatrix} l_1 & l_2 & L \\ m_1 & m_2 & -M \end{pmatrix} \times \begin{pmatrix} l_3 & l_4 & L \\ m_3 & m_4 & M \end{pmatrix} P^{l_1l_2}_{l_3l_4}(L) + (l_2 \leftrightarrow l_3) + (l_2 \leftrightarrow l_4), \quad (8)$$

with

$$P^{l_1l_2}_{l_3l_4}(L) = \mathcal{T}^{l_1l_2}_{l_3l_4}(L) + (-1)^{l_1+l_2+L}\mathcal{T}^{l_2l_1}_{l_3l_4}(L) + (-1)^{l_3+l_4+L}\mathcal{T}^{l_1l_2}_{l_4l_3}(L) + (-1)^{l_1+l_2+l_3+l_4}\mathcal{T}^{l_2l_1}_{l_4l_3}(L), \quad (9)$$

where the factors of powers of (-1) are induced by identities of the Wigner $3j$ symbol. Therefore, we again need only consider the reduced trispectrum $\mathcal{T}$ from one particular arrangement of the multipoles. Indeed, we need only find the reduced CMB trispectrum induced by the reduced primordial trispectrum. In particular, we denote

$$\mathcal{T}_{l_1m_1l_2m_2l_3m_3l_4m_4} = \sum_{LM}(-1)^M \begin{pmatrix} l_1 & l_2 & L \\ m_1 & m_2 & -M \end{pmatrix} \times \begin{pmatrix} l_3 & l_4 & L \\ m_3 & m_4 & M \end{pmatrix} \mathcal{T}^{l_1l_2}_{l_3l_4}(L), \quad (10)$$

and observe that

$$T_{l_1m_1l_2m_2l_3m_3l_4m_4} = \mathcal{T}_{l_1m_1l_2m_2l_3m_3l_4m_4} + \mathcal{T}_{l_2m_2l_1m_1l_3m_3l_4m_4} + \mathcal{T}_{l_1m_1l_2m_2l_4m_4l_3m_3} + \mathcal{T}_{l_2m_2l_1m_1l_4m_4l_3m_3} + \mathcal{T}_{l_1m_1l_3m_3l_2m_2l_4m_4} + \mathcal{T}_{l_3m_3l_1m_1l_2m_2l_4m_4} + \mathcal{T}_{l_1m_1l_3m_3l_4m_4l_2m_2} + \mathcal{T}_{l_3m_3l_1m_1l_4m_4l_2m_2} + \mathcal{T}_{l_1m_1l_4m_4l_2m_2l_3m_3} + \mathcal{T}_{l_4m_4l_1m_1l_2m_2l_3m_3} + \mathcal{T}_{l_1m_1l_4m_4l_3m_3l_2m_2} + \mathcal{T}_{l_4m_4l_1m_1l_3m_3l_2m_2}. \quad (11)$$

B. Relation between the primordial and CMB trispectra

In order to relate the above definitions for the primordial and CMB trispectra, we use the following identities:

$$\delta(\mathbf{k}) = \frac{1}{(2\pi)^3}\int e^{i\mathbf{r}.\mathbf{k}}d^3r, \qquad e^{i\mathbf{r}.\mathbf{k}} = 4\pi\sum_{l,m} i^l j_l(kr)Y_{lm}(\hat{\mathbf{k}})Y^*_{lm}(\hat{\mathbf{r}}), \qquad Y_{l-m} = (-1)^m Y^*_{lm}. \quad (12)$$

We find, using these identities with Eqs. (3) and (4),

$$\mathcal{T}_{l_1m_1l_2m_2l_3m_3l_4m_4} = \left(\frac{2}{\pi}\right)^5(-i)^{\sum l_i}\int(\Pi_{i=1}^4 d^3k_i\Delta_{l_i}(k_i)Y_{l_im_i}(\hat{\mathbf{k}}_i))d^3K\mathcal{T}_\Phi(\mathbf{k}_1,\mathbf{k}_2,\mathbf{k}_3,\mathbf{k}_4;\mathbf{K}) \times \sum_{l'_i,L',L''}\sum_{m'_i,M',M''}\int d^3r_1d^3r_2 i^{\sum l'_i+L'-L''}[j_{l'_1}(k_1r_1)Y_{l'_1m'_1}(\hat{\mathbf{k}}_1)Y^*_{l'_1m'_1}(\hat{\mathbf{r}}_1)][j_{l'_2}(k_2r_1)Y_{l'_2m'_2}(\hat{\mathbf{k}}_2)Y^*_{l'_2m'_2}(\hat{\mathbf{r}}_1)] \times [j_{l'_3}(k_3r_2)Y_{l'_3m'_3}(\hat{\mathbf{k}}_2)Y^*_{l'_3m'_3}(\hat{\mathbf{r}}_2)][j_{l'_4}(k_4r_2)Y_{l'_4m'_4}(\hat{\mathbf{k}}_4)Y^*_{l'_4m'_4}(\hat{\mathbf{r}}_2)][j_{L'}(Kr_1)Y_{L'M'}(\hat{\mathbf{K}})Y^*_{L'M'}(\hat{\mathbf{r}}_1)] \times [j_{L''}(Kr_2)Y^*_{L''M''}(\hat{\mathbf{K}})Y_{L''M''}(\hat{\mathbf{r}}_2)], \quad (13)$$

where $\hat{\mathbf{k}}_i$ represents the unit vector in the direction $\mathbf{k}_i$.

To calculate further, we must choose an appropriate parametrization for $\mathcal{T}_\Phi$. We note that the primordial trispectrum shape has 6 degrees of freedom. We could define the quadrilateral uniquely by the lengths of the four sides $k_i = |\mathbf{k}_i|$, together with the two diagonals $K = |\mathbf{K}|$ and $\tilde{K} = |\tilde{\mathbf{K}}|$. However, we find it more convenient to represent the sixth degree of freedom with the angle θ_4 which represents the deviation of the quadrilateral from planarity (as illustrated in Fig. 2). Using rotational invariance of the trispectrum we may assume that the nonplanarity angle for the $\mathbf{k}_4$ wave vector coincides with θ_4. Many well-

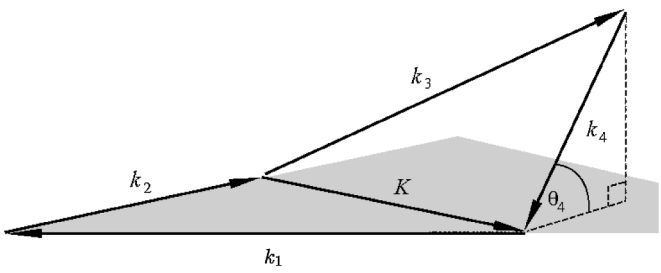

FIG. 2. Quadrilateral defined by the four wave numbers k_i, the diagonal K, and the angle θ_4 out of the plane of the first triangle.

motivated primordial models, such as the local and equilateral cases we shall discuss, are planar (i.e. $\theta_4 = 0$). So we choose the independent parameters to identify the shape to be $(k_1, k_2, k_3, k_4, K, \theta_4)$, that is, $\mathcal{T}_\Phi = \mathcal{T}_\Phi(k_1, k_2, k_3, k_4; K, \theta_4)$. Using this parametrization, the following identities,

$$\int d\Omega_{\hat{r}} Y_{l_1 m_1}(\hat{\mathbf{r}}) Y_{l_2 m_2}(\hat{\mathbf{r}}) Y_{l_3 m_3}(\hat{\mathbf{r}}) = \sqrt{\frac{(2l_1+1)(2l_2+1)(2l_3+1)}{4\pi}} \begin{pmatrix} l_1 & l_2 & l_3 \\ 0 & 0 & 0 \end{pmatrix} \begin{pmatrix} l_1 & l_2 & l_3 \\ m_1 & m_2 & m_3 \end{pmatrix},$$
$$\int d\Omega_{\hat{r}} Y_{lm}(\hat{\mathbf{r}}) Y^*_{l'm'}(\hat{\mathbf{r}}) = \delta_{ll'}\delta_{mm'} \tag{14}$$

and (12), we find

$$\mathcal{T}_{l_1 m_1 l_2 m_2 l_3 m_3 l_4 m_4} = \left(\frac{2}{\pi}\right)^5 \sum_{L', M'} \sum_{l'_4, m'_4} (-1)^{M'} \int (k_1 k_2 k_3 k_4 K)^2 dk_1 dk_2 dk_3 dk_4 dK r_1^2 dr_1 r_2^2 dr_2 j_L(Kr_1) j_L(Kr_2) [j_{l_1}(k_1 r_1)\Delta_{l_1}(k_1)]$$
$$\times [j_{l_2}(k_2 r_1)\Delta_{l_2}(k_2)][j_{l_3}(k_3 r_2)\Delta_{l_3}(k_3)][j_{l_4}(k_4 r_2)\Delta_{l_4}(k_4)] h_{l_1 l_2 L'} h_{l_3 l'_4 L'} (-1)^{m'_4}$$
$$\times \begin{pmatrix} l_1 & l_2 & L' \\ m_1 & m_2 & -M' \end{pmatrix} \begin{pmatrix} l_3 & l'_4 & L' \\ m_3 & -m'_4 & M' \end{pmatrix} \int d\Omega_{\hat{\mathbf{k}}_4} \mathcal{T}_\Phi(k_1, k_2, k_3, k_4; K, \theta_4) Y_{l_4 m_4}(\hat{\mathbf{k}}_4) Y_{l'_4 m'_4}(\hat{\mathbf{k}}_4), \tag{15}$$

where we write

$$h_{l_1 l_2 L'} = \sqrt{\frac{(2l_1+1)(2l_2+1)(2L'+1)}{4\pi}} \begin{pmatrix} l_1 & l_2 & L' \\ 0 & 0 & 0 \end{pmatrix}. \tag{16}$$

Next, we note that inverting Eq. (10) gives the expression

$$\mathcal{T}^{l_1 l_2}_{l_3 l_4}(L) = \sum_{m_i, M} (2L+1)(-1)^M \begin{pmatrix} l_1 & l_2 & L \\ m_1 & m_2 & M \end{pmatrix} \times \begin{pmatrix} l_3 & l_4 & L \\ m_3 & m_4 & -M \end{pmatrix} \mathcal{T}_{l_1 m_1 l_2 m_2 l_3 m_3 l_4 m_4}. \tag{17}$$

The sum over m_1, m_2 is proportional to

$$\sum_{m_1, m_2} (2L+1) \begin{pmatrix} l_1 & l_2 & L \\ m_1 & m_2 & M \end{pmatrix} \begin{pmatrix} l_1 & l_2 & L' \\ m_1 & m_2 & -M' \end{pmatrix} = \delta_{L,L'}\delta_{M,-M'} \tag{18}$$

and therefore the sum over L', M' implies $L' = L$ and $M' = -M$. The sum over m_3, M is then proportional to

$$\sum_{m_3, M} \begin{pmatrix} l_3 & l_4 & L \\ m_3 & m_4 & -M \end{pmatrix} \begin{pmatrix} l_3 & l'_4 & L \\ m_3 & -m'_4 & -M \end{pmatrix} = \frac{1}{2l'_4+1} \delta_{l_4, l'_4} \delta_{m_4, -m'_4}. \tag{19}$$

Combining these we find that

$$\mathcal{T}^{l_1 l_2}_{l_3 l_4}(L) = h_{l_1 l_2 L} h_{l_3 l_4 L} \left(\frac{2}{\pi}\right)^5 \int (k_1 k_2 k_3 k_4 K)^2 dk_1 dk_2 dk_3 dk_4 dK r_1^2 dr_1 r_2^2 dr_2 j_L(Kr_1) j_L(Kr_2) [j_{l_1}(k_1 r_1)\Delta_{l_1}(k_1)]$$
$$\times [j_{l_2}(k_2 r_1)\Delta_{l_2}(k_2)][j_{l_3}(k_3 r_2)\Delta_{l_3}(k_3)][j_{l_4}(k_4 r_2)\Delta_{l_4}(k_4)] \frac{1}{2l_4+1}$$
$$\times \sum_{m_4 = -l_4}^{l_4} \int d\Omega_{\hat{\mathbf{k}}_4} \mathcal{T}_\Phi(k_1, k_2, k_3, k_4; K, \theta_4) Y_{l_4 m_4}(\hat{\mathbf{k}}_4) Y^*_{l_4 m_4}(\hat{\mathbf{k}}_4). \tag{20}$$

We can decompose this expression further by expanding the primordial trispectrum as a Legendre series. In particular, we write

$$\mathcal{T}_\Phi(k_1, k_2, k_3, k_4; K, \theta_4) = \sum_{n=0}^{\infty} \mathcal{T}_{\Phi, n}(k_1, k_2, k_3, k_4; K) P_n(\cos\theta_4). \tag{21}$$

This is an expansion about the $n = 0$ planar mode which, as we have noted, is sufficient for describing many well-motivated models. Noting that $P_n = \sqrt{\frac{4\pi}{2n+1}} Y_{n0}$, our expression for the CMB trispectrum becomes

$$\mathcal{T}^{l_1 l_2}_{l_3 l_4}(L) = h_{l_1 l_2 L} h_{l_3 l_4 L} \left(\frac{2}{\pi}\right)^5 \int (k_1 k_2 k_3 k_4 K)^2 dk_1 dk_2 dk_3 dk_4 dK r_1^2 dr_1 r_2^2 dr_2 j_L(Kr_1) j_L(Kr_2) [j_{l_1}(k_1 r_1)\Delta_{l_1}(k_1)]$$
$$\times [j_{l_2}(k_2 r_1)\Delta_{l_2}(k_2)][j_{l_3}(k_3 r_2)\Delta_{l_3}(k_3)][j_{l_4}(k_4 r_2)\Delta_{l_4}(k_4)] \sum_{m_4=-l_4}^{l_4} \sum_{n=0}^{\infty} (-1)^{m_4} \begin{pmatrix} l_4 & l_4 & n \\ 0 & 0 & 0 \end{pmatrix}$$
$$\times \begin{pmatrix} l_4 & l_4 & n \\ m_4 & -m_4 & 0 \end{pmatrix} \mathcal{T}_{\Phi,n}(k_1, k_2, k_3, k_4; K).$$

This expression may be further simplified by noting

$$\sum_{m_4} (-1)^{m_4} \begin{pmatrix} l_4 & l_4 & n \\ m_4 & -m_4 & 0 \end{pmatrix} = (-1)^{l_4} \sqrt{2l_4 + 1}\, \delta_{n0}$$

and

$$\begin{pmatrix} l_4 & l_4 & 0 \\ 0 & 0 & 0 \end{pmatrix} = (-1)^{l_4} \frac{1}{\sqrt{2l_4 + 1}},$$

which together imply that the final line reduces to $\mathcal{T}_{\Phi,0}$. In particular, we have

$$\mathcal{T}^{l_1 l_2}_{l_3 l_4}(L) = h_{l_1 l_2 L} h_{l_3 l_4 L} \left(\frac{2}{\pi}\right)^5 \int (k_1 k_2 k_3 k_4 K)^2 dk_1 dk_2 dk_3 dk_4 dK r_1^2 dr_1 r_2^2 dr_2 j_L(Kr_1) j_L(Kr_2) [j_{l_1}(k_1 r_1)\Delta_{l_1}(k_1)]$$
$$\times [j_{l_2}(k_2 r_1)\Delta_{l_2}(k_2)][j_{l_3}(k_3 r_2)\Delta_{l_3}(k_3)][j_{l_4}(k_4 r_2)\Delta_{l_4}(k_4)] \mathcal{T}_{\Phi,0}(k_1, k_2, k_3, k_4; K). \quad (22)$$

The reduction to the $n = 0$ mode in (22) shows clearly that the CMB only probes and constrains the planar component of the primordial trispectrum T_Φ. In order to test theories which have general nonplanar $n > 0$ contributions, we will have to use 3D data, such as 21 cm surveys or large-scale galaxy distributions (as we shall discuss later).

From Eq. (20) it is clear that the definition-reduced trispectrum [34] includes an unnecessary geometrical factor $h_{l_1 l_2 L} h_{l_3 l_4 L}$, and we therefore advocate the use of the true reduced trispectrum,

$$t^{l_1 l_2}_{l_3 l_4}(L) = \frac{\mathcal{T}^{l_1 l_2}_{l_3 l_4}(L)}{h_{l_1 l_2 L} h_{l_3 l_4 L}}, \quad (23)$$

by analogy with the reduced bispectrum $b_{l_1 l_2 l_3} = B_{l_1 l_2 l_3}/h_{l_1 l_2 l_3}$, where $B_{l_1 l_2 l_3}$ represents the angle-averaged bispectrum. To prevent confusion, however, we refer to $t^{l_1 l_2}_{l_3 l_4}(L)$ as the "extra"-reduced trispectrum.

C. Relationship between the primordial trispectrum and other probes

As is clear from Eq. (22) the CMB trispectrum depends only on the zeroth Legendre mode of the primordial trispectrum. Therefore, in order to break this degeneracy other probes of non-Gaussianity should be considered. As has been discussed in [35] the matter density perturbations are related to the primordial fluctuations by the Poisson equation via the expression

$$\delta_{\mathbf{k}}(a) = M(k; a)\Phi_{\mathbf{k}}, \quad (24)$$

where a is the scale factor and $M(k; a)$ is given by

$$M(k; a) = -\frac{3}{5} \frac{k^2 T(k)}{\Omega_m H_0^2} D_+(a), \quad (25)$$

where $T(k)$ is the transfer function, $D_+(a)$ is the growth factor in linear perturbation theory, Ω_m is the present value of the dark matter density, and H_0 is the present value of the Hubble constant. Therefore, the primordial contribution to the n-point connected correlation function of matter density perturbations at a given value of the scale factor is given by

$$\langle \delta_{\mathbf{k}_1}(a)\delta_{\mathbf{k}_2}(a) \ldots \delta_{\mathbf{k}_n}(a)\rangle_c = M(k_1; a)M(k_2; a) \ldots M(k_n; a)\langle \Phi_{\mathbf{k}_1}\Phi_{\mathbf{k}_2} \ldots \Phi_{\mathbf{k}_n}\rangle_c. \quad (26)$$

Possible probes of the matter density perturbations include galaxy surveys and the Lyman alpha forest, i.e. the sum of absorption lines from the Ly-α transition of the neutral hydrogen in the spectra of distant galaxies and quasars. There are three sources of non-Gaussianity in such surveys [36]: one primordial, one due to gravitational instability, and the last due to nonlinear bias. The 21 cm observations offer another probe of non-Gaussianity and are less subject to the unknown galaxy bias, especially at high redshift. However, uncertainties in the neutral fraction replace the uncertainties in the bias in this case. There are also complications due to redshift space distortions arising from peculiar velocities. Despite these drawbacks, recent advances in this area suggest that probes of the matter density perturbations potentially represent a powerful tool to detect non-Gaussianity and possibly break the degeneracy implicit in trispectrum measurements using the CMB. The study of such data involves using the full Legendre expan-

sion of the primordial trispectrum as in Eq. (21). In the remainder of this paper we proceed to investigate the CMB trispectrum. However, many of the results presented in the paper are straightforwardly extended to alternative probes of non-Gaussianity as discussed here.

D. Ideal estimator

Unfortunately, the trispectrum signal, like the bispectrum, is too weak for us to measure individual multipoles directly. Therefore, in order to compare theory with observations it is necessary to use an estimator that sums over all multipoles. Estimators can be thought of as performing a least-squares fit of the trispectrum predicted by theory, $\langle a_{l_1m_1}a_{l_2m_2}a_{l_3m_3}a_{l_4m_4}\rangle_c$, to the trispectrum obtained from observations. The trispectrum from observations is given by $(a^{\rm obs}_{l_1m_1}a^{\rm obs}_{l_2m_2}a^{\rm obs}_{l_3m_3}a^{\rm obs}_{l_4m_4})_c$, where we subtract the unconnected or Gaussian part, denoted uc, from the four-point function, $a^{\rm obs}_{l_1m_1}a^{\rm obs}_{l_2m_2}a^{\rm obs}_{l_3m_3}a^{\rm obs}_{l_4m_4}$. This unconnected part is related to the observed angular power spectrum $C^{\rm obs}_l$ by

$$(a^{\rm obs}_{l_1m_1}a^{\rm obs}_{l_2m_2}a^{\rm obs}_{l_3m_3}a^{\rm obs}_{l_4m_4})_{\rm uc} = (-1)^{m_1+m_3}C^{\rm obs}_{l_1}C^{\rm obs}_{l_3}\delta_{l_1,l_2}\delta_{m_1,-m_2}\delta_{l_3,l_4}\delta_{m_3,-m_4} + (-1)^{m_1+m_2}C^{\rm obs}_{l_1}C^{\rm obs}_{l_2}(\delta_{l_1,l_3}\delta_{m_1,-m_3}\delta_{l_2,l_4}\delta_{m_2,-m_4} + \delta_{l_1,l_4}\delta_{m_1,-m_4}\delta_{l_2,l_3}\delta_{m_2,-m_3}). \quad (27)$$

We define the estimator to be

$$\mathcal{E} = \frac{1}{N_T}\sum_{l_im_i}\frac{\langle a_{l_1m_1}a_{l_2m_2}a_{l_3m_3}a_{l_4m_4}\rangle_c(a^{\rm obs}_{l_1m_1}a^{\rm obs}_{l_2m_2}a^{\rm obs}_{l_3m_3}a^{\rm obs}_{l_4m_4})_c}{C_{l_1}C_{l_2}C_{l_3}C_{l_4}}, \quad (28)$$

where the normalization factor N_T is given by (see Appendix A)

$$N_T = \sum_{l_i,L}\frac{T^{l_1l_2}_{l_3l_4}(L)T^{l_1l_2}_{l_3l_4}(L)}{(2L+1)C_{l_1}C_{l_2}C_{l_3}C_{l_4}}. \quad (29)$$

As is clear from the earlier discussion, assuming isotropy for a given theoretical model, we need only calculate the reduced trispectrum $\mathcal{T}^{l_1l_2}_{l_3l_4}(L)$, rather than the more challenging full trispectrum $\langle a_{l_1m_1}a_{l_2m_2}a_{l_3m_3}a_{l_4m_4}\rangle_c$.

This estimator naturally defines a correlator for testing whether two competing trispectra could be differentiated by an ideal experiment. Replacing the observed trispectrum with one calculated from a competing theory, we have

$$\mathcal{C}(T,T') = \frac{1}{N_T}\sum_{l_i,m_i}\frac{\langle a_{l_1m_1}a_{l_2m_2}a_{l_3m_3}a_{l_4m_4}\rangle_c\langle a'_{l_1m_1}a'_{l_2m_2}a'_{l_3m_3}a'_{l_4m_4}\rangle_c}{C_{l_1}C_{l_2}C_{l_3}C_{l_4}} = \frac{1}{N_T}\sum_{l_i,L}\frac{T^{l_1l_2}_{l_3l_4}(L)T'^{l_1l_2}_{l_3l_4}(L)}{(2L+1)C_{l_1}C_{l_2}C_{l_3}C_{l_4}}, \quad (30)$$

where now the normalization N_T is defined as follows,

$$N_T = \sqrt{\sum_{l_i,L}\frac{T^{l_1l_2}_{l_3l_4}(L)T^{l_1l_2}_{l_3l_4}(L)}{(2L+1)C_{l_1}C_{l_2}C_{l_3}C_{l_4}}}\sqrt{\sum_{l_i,L}\frac{T'^{l_1l_2}_{l_3l_4}(L)T'^{l_1l_2}_{l_3l_4}(L)}{(2L+1)C'_{l_1}C'_{l_2}C'_{l_3}C'_{l_4}}}. \quad (31)$$

An alternative correlator between two trispectra, which is easier to solve numerically, is found by replacing the trispectra by the respective reduced trispectra in the above definitions. Therefore, when comparing two trispectra we shall use this latter definition, $\mathcal{C}(\mathcal{T},\mathcal{T}')$. The exact relation between the two correlators can be deduced from Appendix B in Ref. [34].

E. General estimator

The above estimator is applicable for general trispectra in the limit where non-Gaussianity is small and the observed map is free of instrument noise and foreground contamination. Of course, this is an idealized case and we need to consider taking into account the effect of sky cuts and inhomogeneous noise. Here we follow the approach of [37] (an approach that is further elucidated in [38,39]). As we prove in Appendix B the appropriate form of the optimal estimator becomes

$$\mathcal{E}^{\rm general} = \frac{f_{\rm sky}}{\tilde{N}}\sum_{l_im_i}\langle a_{l_1m_1}a_{l_2m_2}a_{l_3m_3}a_{l_4m_4}\rangle_c[(C^{-1}a^{\rm obs})_{l_1m_1}(C^{-1}a^{\rm obs})_{l_2m_2}(C^{-1}a^{\rm obs})_{l_3m_3}(C^{-1}a^{\rm obs})_{l_4m_4} - 6(C^{-1})_{l_1m_1,l_2m_2} \times (C^{-1}a^{\rm obs})_{l_3m_3}(C^{-1}a^{\rm obs})_{l_4m_4} + 3(C^{-1})_{l_1m_1,l_2m_2}(C^{-1})_{l_3m_3,l_4m_4}], \quad (32)$$

where

$$\tilde{N} = \sum_{l_i m_i} \langle a_{l_1 m_1} a_{l_2 m_2} a_{l_3 m_3} a_{l_4 m_4} \rangle_c (C^{-1})_{l_1 m_1, l_1' m_1'} (C^{-1})_{l_2 m_2, l_2' m_2'} (C^{-1})_{l_3 m_3, l_3' m_3'} (C^{-1})_{l_4 m_4, l_4' m_4'} \langle a_{l_1' m_1'} a_{l_2' m_2'} a_{l_3' m_3'} a_{l_4' m_4'} \rangle_c,$$

$f_{\rm sky}$ is the fraction of the sky outside the mask, and where the covariance matrix C is now nondiagonal due to mode-mode coupling introduced by the mask and anisotropic noise. Because of the breaking of isotropy extra terms have been added in order to maintain the optimality of the estimator. The optimal estimator, in the case that the covariance matrix is diagonal, reads

$$\mathcal{E} = \frac{f_{\rm sky}}{N_T} \sum_{l_i m_i} \frac{\langle a_{l_1 m_1} a_{l_2 m_2} a_{l_3 m_3} a_{l_4 m_4} \rangle_c}{C_{l_1} C_{l_2} C_{l_3} C_{l_4}} [a^{\rm obs}_{l_1 m_1} a^{\rm obs}_{l_2 m_2} a^{\rm obs}_{l_3 m_3} a^{\rm obs}_{l_4 m_4} - 6(-1)^{m_1} C_{l_1} \delta_{l_1 l_2} \delta_{m_1 - m_2} a^{\rm obs}_{l_3 m_3} a^{\rm obs}_{l_4 m_4} + 3(-1)^{m_1 + m_2} \delta_{l_1 l_2} \delta_{m_1 - m_2} \delta_{l_3 l_4} \delta_{m_3 - m_4} C_{l_1} C_{l_3}], \tag{33}$$

where N_T is given by Eq. (29). We note also that the average of this estimator is

$$\langle \mathcal{E} \rangle = \frac{f_{\rm sky}}{N_T} \sum_{l_i m_i} \frac{\langle a_{l_1 m_1} a_{l_2 m_2} a_{l_3 m_3} a_{l_4 m_4} \rangle_c \langle a^{\rm obs}_{l_1 m_1} a^{\rm obs}_{l_2 m_2} a^{\rm obs}_{l_3 m_3} a^{\rm obs}_{l_4 m_4} \rangle_c}{C_{l_1} C_{l_2} C_{l_3} C_{l_4}}, \tag{34}$$

as expected.

In the remainder of this paper we shall refer to the ideal estimator, unless otherwise stated. However, this formula is important for the general implementation of the formalisms introduced here.

F. Kurtosis as a measure of non-Gaussianity

As an aside, we note that the use of nonoptimal estimators may also provide useful information, e.g. as a reality check on these complex calculations. The kurtosis of the one-point temperature distribution offers such an estimator. The kurtosis g_2 is defined as

$$g_2 = \frac{\langle (\frac{\Delta T}{T}(\hat{n}))^4 \rangle}{(\langle (\frac{\Delta T}{T}(\hat{n}))^2 \rangle)^2} - 3. \tag{35}$$

As we show in Appendix C (where we also include a discussion on the skewness for completeness) the kurtosis may be written in the following form:

$$g_2 = \frac{48\pi \sum_{l_i, L} h^2_{l_1 l_2 L} h^2_{l_3 l_4 L} t^{l_1 l_2}_{l_3 l_4}(L)/(2L+1)}{(\sum_l (2l+1) C_l)^2}. \tag{36}$$

The calculation of this quantity is relatively straightforward compared to the full estimator due to the absence of Wigner $6j$ symbols in the expression.

III. THE SHAPE OF PRIMORDIAL TRISPECTRA

A. Shape function

It is known from CMB observations that the power spectrum is nearly scale invariant. An analysis of the bispectrum is performed using the shape function, which is a scale-invariant form of the bispectrum. To parallel this analysis we wish to write a scale-invariant form of the trispectrum (or, in particular, the trispectrum modes). Therefore, we need to eliminate a k^9 scaling. Motivated by (22) we define this shape by

$$S_T(k_1, k_2, k_3, k_4, K) = \frac{(k_1 k_2 k_3 k_4)^2 K}{\Delta^3_\Phi N} T_{\Phi,0}(k_1, k_2, k_3, k_4; K), \tag{37}$$

where N is an appropriate normalization factor. For clarity, in what follows we shall use the symbol $S_{\mathcal{T}}$ when referring to the shape induced by the reduced primordial trispectrum. Of course, this choice of the shape function is not unique. Another choice of shape function is

$$\tilde{S}_T(k_1, k_2, k_3, k_4, K) = \frac{(k_1 k_2 k_3 k_4)^{9/4}}{\Delta^3_\Phi N} T_{\Phi,0}(k_1, k_2, k_3, k_4; K), \tag{38}$$

which has the advantage of remaining independent of the diagonal K if the underlying trispectrum has this property. Such a class of models is discussed further in Appendix D. Nonetheless, we proceed with S_T as our choice of shape function in this paper, leaving further investigation of this issue to a future publication [40]. We should also notice that, since our analysis here is focused on the CMB, we have only included the zeroth mode of the Legendre expansion as indicated by (22). However, for more general probes of non-Gaussianity, as discussed in Sec. II, the full Legendre expansion described by Eq. (21) is required. In such a case the analysis outlined here can be applied mode by mode. Because of orthogonality of the Legendre modes, extending the study is a trivial task.

If we rewrite the reduced CMB trispectrum in terms of the shape function $S_{\mathcal{T}}$, we have

$$\mathcal{T}^{l_1 l_2}_{l_3 l_4}(L) = N h_{l_1 l_2 L} h_{l_3 l_4 L} \left(\frac{2}{\pi}\right)^5 \int d\mathcal{V}_k S_{\mathcal{T}}(k_1, k_2, k_3, k_4, K) \times K \Delta_{l_1}(k_1) \Delta_{l_2}(k_2) \Delta_{l_3}(k_3) \Delta_{l_4}(k_4) \times I^G_{l_1 l_2 l_3 l_4 L}(k_1, k_2, k_3, k_4, K), \tag{39}$$

where the integral I^G is given by

$$I^G_{l_1 l_2 l_3 l_4 L}(k_1, k_2, k_3, k_4, K) = \int r_1^2 r_2^2 dr_1 dr_2 j_L(Kr_1) j_L(Kr_2) \times j_{l_1}(k_1 r_1) j_{l_2}(k_2 r_1) j_{l_3}(k_3 r_2) \times j_{l_4}(k_4 r_2) \quad (40)$$

and $d\mathcal{V}_k$ corresponds to the area inside the region $k_i, K/2 \in [0, k_{\rm max}]$ allowed by the triangle conditions. Therefore, the shape function is the signal that is evolved via the transfer functions to give the trispectrum today. Essentially, I^G acts like a window function on all the shapes as it projects from k to l space; that is, it will tend to smear out their sharper distinguishing features. This means that the shape function $S_{\mathcal{T}}$, especially in the scale-invariant case, can be thought of as the primordial counterpart of the reduced CMB trispectrum $\mathcal{T}^{l_1 l_2}_{l_3 l_4}(L)$ before projection.

B. Shape correlators

We wish to construct a primordial shape correlator that predicts the value of the CMB correlator $\mathcal{C}(\mathcal{T}, \mathcal{T}')$. To this end we should consider something of the form

$$F(S_{\mathcal{T}}, S_{\mathcal{T}'}) = \int d\mathcal{V}_k S_{\mathcal{T}}(k_1, k_2, k_3, k_4, K) \times S_{\mathcal{T}'}(k_1, k_2, k_3, k_4, K) \omega(k_1, k_2, k_3, k_4, K), \quad (41)$$

where ω is an appropriate weight function. With this choice of weight the primordial shape correlator then takes the form

$$\bar{\mathcal{C}}(S_{\mathcal{T}}, S_{\mathcal{T}'}) = \frac{F(S_{\mathcal{T}}, S_{\mathcal{T}'})}{\sqrt{F(S_{\mathcal{T}}, S_{\mathcal{T}}) F(S_{\mathcal{T}'}, S_{\mathcal{T}'})}}. \quad (42)$$

The question now is what weight function should we choose? Our goal is to choose $S^2\omega$ in k space such that it produces the same scaling as the estimator $T^2/((2L + 1)C^4)$ in l space. Let us consider the simplest case where $k = k_1 = k_2 = k_3 = k_4 = K$ and $l = l_1 = l_2 = l_3 = l_4 = L$. For primordial trispectra which are scale invariant, we then have

$$S^2_{\mathcal{T}}(k, k, k, k, k)\omega(k, k, k, k, k) \propto \omega(k, k, k, k, k). \quad (43)$$

If we work in the large-angle approximation, and assume $l + 1 \approx l$, then we know $C_l \propto l^{-2}$, and from the analytic solution for the local model, which we will describe below [see Eqs. (59) and (63)], we have

$$T^{ll}_{ll}(l) \propto h^2_{lll} \frac{1}{l^6}. \quad (44)$$

Now

$$h_{lll} \propto l^{3/2} \begin{pmatrix} l & l & l \\ 0 & 0 & 0 \end{pmatrix}$$

and the Wigner $3J$ symbol has an exact solution for which

$$\begin{pmatrix} l & l & l \\ 0 & 0 & 0 \end{pmatrix} \approx (-1)^{3l/2} \frac{1}{\sqrt{3l+1}} \sqrt{\frac{l!^3}{3l!}} \frac{(3l/2)!}{(l/2)!^3} \approx (-1)^{3l/2} \sqrt{\frac{2}{\sqrt{3}\pi}} \frac{1}{l}. \quad (45)$$

Therefore $T^{ll}_{ll}(l) \propto l^{-5}$ and so

$$\frac{T^{ll}_{ll}(l)^2}{(2l+1)C_l^4} \propto l^{-3}. \quad (46)$$

Hence we find that we should choose a weight function $\omega(k, k, k, k, k) \propto k^{-3}$. The particular choice of ω may significantly improve forecasting accuracy—by, for instance, using a phenomenological window function to incorporate damping due to photon diffusion or smoothing due to projection from k to l space—but it does not impact important qualitative insights. A specific choice of weight function, motivated by the choice of weight function for the bispectrum, is the following:

$$w(k_1, k_2, k_3, k_4, K) = \frac{K}{(k_1 + k_2 + K)^2 (k_3 + k_4 + K)^2}. \quad (47)$$

C. Shape decomposition

Given the strong observational limits on the scalar tilt, we expect all shape functions to exhibit behavior close to scale invariance, so that $S_{\mathcal{T}}(k_1, k_2, k_3, k_4, K)$ will depend only weakly on the overall magnitude of the summed wave numbers. Here we choose to parametrize the magnitude of the wave numbers with the quantity

$$k = \tfrac{1}{2}(k_1 + k_2 + K). \quad (48)$$

k is the semiperimeter of the triangle formed by the vectors $\mathbf{k_1}, \mathbf{k_2}, \mathbf{K}$. Because of the scaling behavior the form of the shape function on a cross section is essentially independent of k, so that

$$S_{\mathcal{T}}(k_1, k_2, k_3, k_4, K) = f(k)\bar{S}_{\mathcal{T}}(\hat{k}_1, \hat{k}_2, \hat{k}_3, \hat{k}_4, \hat{K}), \quad (49)$$

where $\hat{k}_i = k_i/k$ and $\hat{K} = K/k$. Since we are restricted to the region where the wave numbers (k_1, k_2, K) and (k_3, k_4, K) form triangles by momentum conservation, we will reparametrize the allowed region to separate out the overall scale k from the behavior on a cross-sectional slice. This four-dimensional slice is spanned by the remaining coordinates. Concentrating on each triangle individually, we reparametrize in a similar fashion to the analysis done in [3]. For triangle (k_1, k_2, K) we have

$$K = k(1 - \beta), \qquad k_1 = \frac{k}{2}(1 + \alpha + \beta), \qquad k_2 = \frac{k}{2}(1 - \alpha + \beta), \quad (50)$$

while for triangle (k_3, k_4, K) we have

$$K = \epsilon k(1-\delta), \qquad k_3 = \frac{\epsilon k}{2}(1+\gamma+\delta), \qquad k_4 = \frac{\epsilon k}{2}(1-\gamma+\delta), \tag{51}$$

where ϵ parametrizes the ratio of the perimeters of the two triangles, i.e. $\epsilon = \frac{k_3+k_4+K}{k_1+k_2+K}$. We consider $1 \le \epsilon < \infty$. The different expressions for K imply that

$$1-\beta = \epsilon(1-\delta). \tag{52}$$

The conditions for triangle (k_1, k_2, K) that $0 \le k_1, k_2, K \le k$ imply that $0 \le \beta \le 1$ and $-(1-\beta) \le \alpha \le 1-\beta$, while the conditions for triangle (k_3, k_4, K) that $0 \le k_1, k_2, K \le \epsilon k$, along with the relationship between δ and β and the requirement that $\epsilon \ge 1$, imply that $-(1-\beta)/\epsilon \le \gamma \le (1-\beta)/\epsilon$. In summary, we have the following domains,

$$0 \le k < \infty, \qquad 1 \le \epsilon < \infty, \qquad 0 \le \beta \le 1, \qquad -(1-\beta) \le \alpha \le 1-\beta, \qquad -\frac{1-\beta}{\epsilon} \le \gamma \le \frac{1-\beta}{\epsilon}. \tag{53}$$

With this parametrization we can rewrite the shape function and the volume element, respectively, as

$$S_{\mathcal{T}}(k_1, k_2, k_3, k_4, K) = f(k)\bar{\mathcal{S}}_{\mathcal{T}}(\alpha, \beta, \gamma, \epsilon), \qquad d\mathcal{V}_k = dk_1 dk_2 dk_3 dk_4 dK = \epsilon k^4 dk d\alpha d\beta d\gamma d\epsilon. \tag{54}$$

In order to represent the shape function graphically we can choose fixed values of ϵ, in which case the shape $\bar{\mathcal{S}}$ becomes three dimensional. The particular three-dimensional domain is shown in Fig. 3. From the image we see how the particular triangles created by the wave numbers generate the three-dimensional slice for each ϵ. We can envisage the four-dimensional shape by imagining an orthogonal direction for ϵ out of the page, along which are located increasingly squeezed rectangular pyramids.

IV. SEPARABLE SHAPES

A. Examples: Local, equilateral, and constant models

The local model is given by the reduced primordial trispectrum

$$\mathcal{T}^{\rm loc}_{\Phi}(\mathbf{k}_1, \mathbf{k}_2, \mathbf{k}_3, \mathbf{k}_4; \mathbf{K}) = \mathcal{T}^{\rm loc}_{\Phi A}(\mathbf{k}_1, \mathbf{k}_2, \mathbf{k}_3, \mathbf{k}_4; \mathbf{K}) + \mathcal{T}^{\rm loc}_{\Phi B}(\mathbf{k}_1, \mathbf{k}_2, \mathbf{k}_3, \mathbf{k}_4; \mathbf{K}), \tag{55}$$

where

$$\mathcal{T}^{\rm loc}_{\Phi A}(\mathbf{k}_1, \mathbf{k}_2, \mathbf{k}_3, \mathbf{k}_4; \mathbf{K}) = \frac{25}{9}\tau_{NL} P_\Phi(K) P_\Phi(k_1) P_\Phi(k_3), \tag{56}$$

$$\mathcal{T}^{\rm loc}_{\Phi B}(\mathbf{k}_1, \mathbf{k}_2, \mathbf{k}_3, \mathbf{k}_4; \mathbf{K}) = g_{NL}[P_\Phi(k_2)P_\Phi(k_3)P_\Phi(k_4) + P_\Phi(k_1)P_\Phi(k_2)P_\Phi(k_4)]. \tag{57}$$

For single-field inflation we have $\tau_{NL} = (\frac{6}{5} f_{NL})^2$. This relationship breaks down for multifield inflation (see [41]). We can see clearly here that the local trispectrum is independent of the angle θ_4; i.e. the zeroth mode of the local trispectrum is exactly the full local trispectrum. The primordial shapes for each of these expressions may be shown visually using the prescription described in the previous section, and they are shown in Figs. 4 and 5. As expected, for the local model the signal peaks in the corners. However, as is easily observable, the "peaking" behavior is somewhat orthogonal between the two models. Working in the Sachs-Wolfe approximation, where we replace the transfer function with a Bessel function,

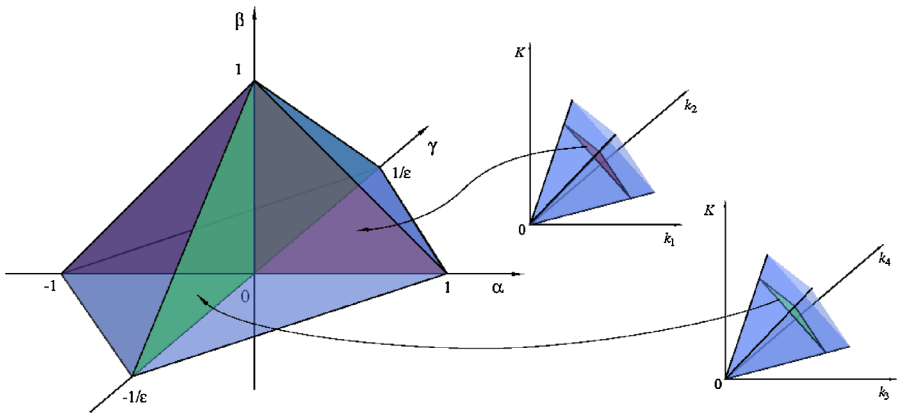

FIG. 3 (color online). Three-dimensional shape function domain for a fixed value of ϵ, i.e. for a particular ratio of the perimeters of the triangles created by the wave numbers (k_1, k_2, K) and (k_3, k_4, K), respectively. Note that the triangle conditions on these two wave number sets restrict them to the two tetrahedral domains illustrated (right diagrams). Slices through these tetrahedra are mapped, as shown, into the full domain, a rectangular pyramid (left diagram).

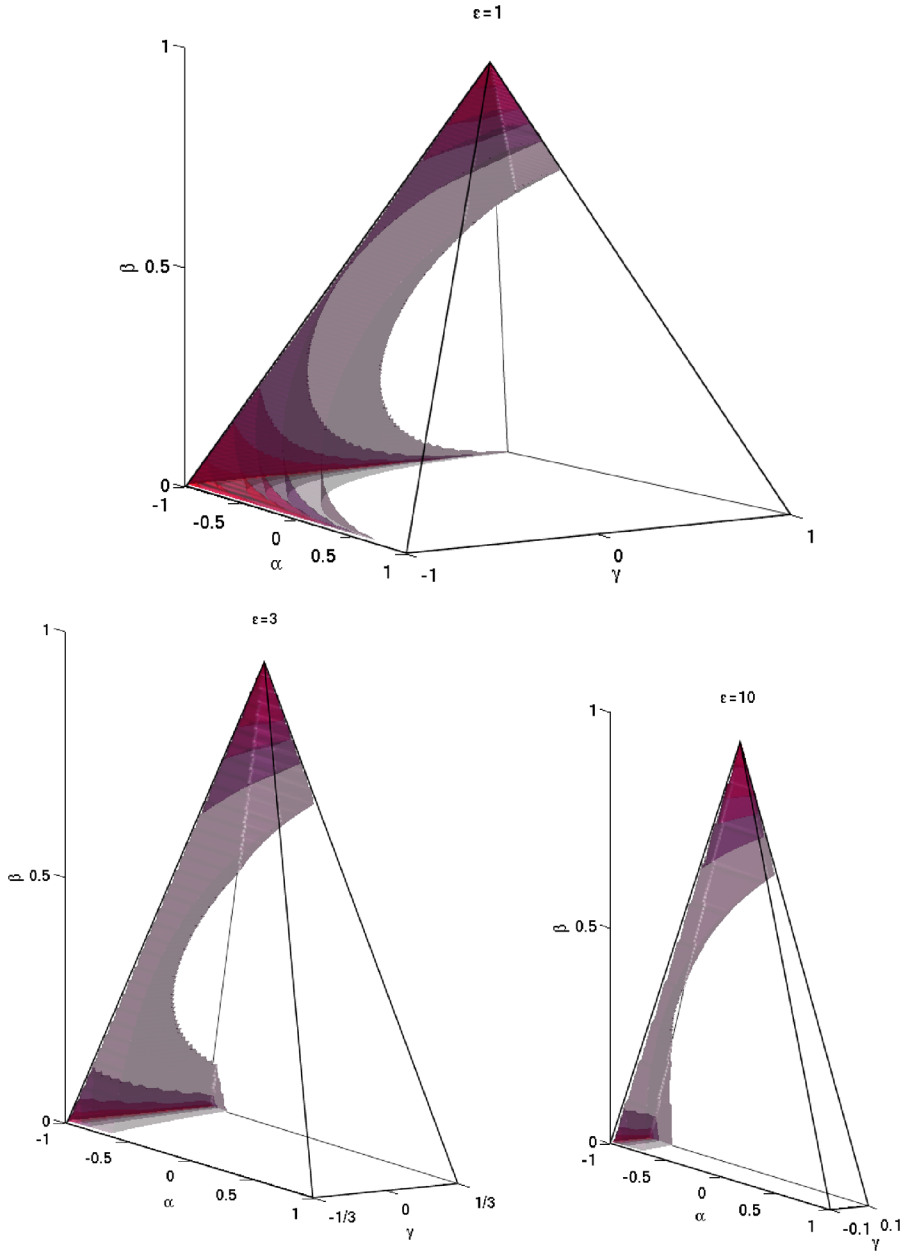

FIG. 4 (color online). Local A model (59). The peak as $\beta \to 1$ corresponds to $K \to 0$, i.e. the "doubly squeezed" limit. The other peak corresponds to $k_1 \to 0$, $k_3 \to (\epsilon - 1)k$. As ϵ rises above unity [i.e. for triangle (k_3, k_4, K) bigger than triangle (k_1, k_2, K)] we expect this peak to become suppressed, as observed.

$$\Delta_l(k) = \tfrac{1}{3} j_l((\tau_0 - \tau_{\rm dec})k), \tag{58}$$

the integral for the reduced trispectrum can be expressed in closed form. Setting $P_\Phi(k) = \Delta_\Phi k^{-3}$ we find

$$\begin{aligned}
\mathcal{T}^{l_1 l_2 \rm loc}_{l_3 l_4, A}(L) &= \frac{25\tau_{NL}}{9}\frac{\Delta_\Phi^3}{3^4}\left(\frac{2}{\pi}\right)^5 h_{l_1 l_2 L} h_{l_3 l_4 L} \int r_1^2 dr_1 r_2^2 dr_2 K^{-1} dK k_1^{-1} dk_1 k_3^{-1} dk_3 I_{l_2}(2, r_1) I_{l_4}(2, r_1) \\
&= \frac{25\tau_{NL}}{9}\frac{\Delta_\Phi^3}{3^4}\left(\frac{2}{\pi}\right)^5 h_{l_1 l_2 L} h_{l_3 l_4 L}\left(\frac{\pi}{2}\right)^2 I_L(-1, 1) I_{l_1}(-1, 1) I_{l_3}(-1, 1) \\
&= \frac{25\tau_{NL}}{36}\pi^2\frac{\Delta_\Phi^3}{3^4}\left(\frac{2}{\pi}\right)^5 h_{l_1 l_2 L} h_{l_3 l_4 L}\left(\frac{1}{2L(L+1)2l_1(l_1+1)2l_3(l_3+1)}\right),
\end{aligned} \tag{59}$$

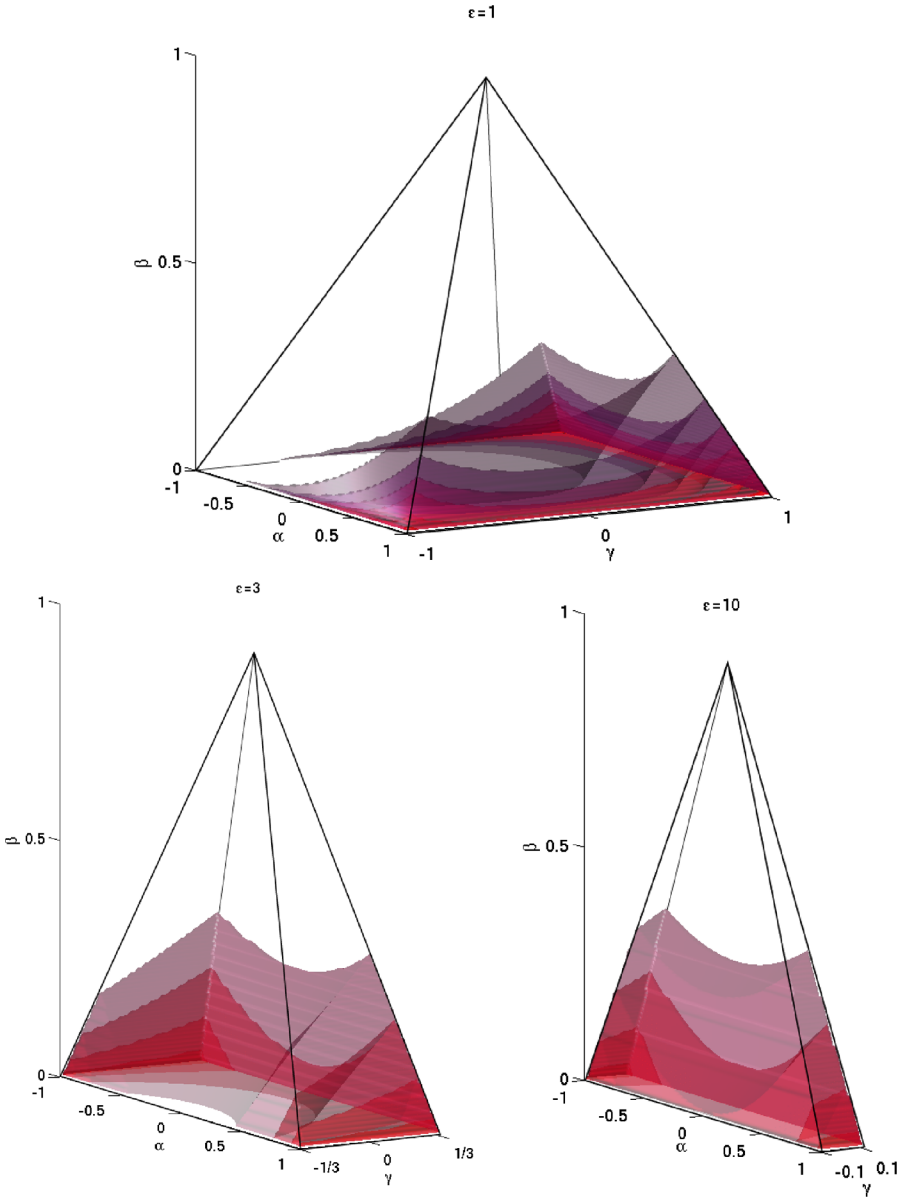

FIG. 5 (color online). Local B model (63). The peaks at $\alpha = 1$ correspond to $k_2 \to 0$, while the peaks at $\alpha = -1$ correspond to $k_1 \to 0$. For $\epsilon = 1$ [i.e. equal triangle sizes (k_1, k_2, K) and (k_3, k_4, K)] we see a more confined peaking at $\gamma = -1$, $\gamma = 1$, i.e. $k_3 \to 0$, $k_4 \to 0$, respectively. We observe the peaking of the local B models to be somewhat orthogonal to the local A model.

where

$$I_l(p, x) = \int k^p dk j_l(k) j_l(xk), \tag{60}$$

and we have used

$$I_l(2, r) = \frac{\pi}{2r^2}\delta(r - 1), \tag{61}$$

$$I_l(-1, 1) = \frac{1}{2l(l + 1)}. \tag{62}$$

Similarly,

$$\mathcal{T}^{l_1 l_2 \mathrm{loc}}_{l_3 l_4, B}(L) = g_{NL}\frac{\pi^2}{4}\frac{\Delta^3_\Phi}{3^4}\left(\frac{2}{\pi}\right)^5 h_{l_1 l_2 L} h_{l_3 l_4 L} \times \left(\frac{1}{2l_2(l_2 + 1)2l_3(l_3 + 1)2l_4(l_4 + 1)} + (l_1 \leftrightarrow l_3)\right). \tag{63}$$

Next we propose a *constant* model for the primordial trispectrum, analogous to the simplest model for the bispectrum. This is given by

$$\frac{1}{\Delta_\Phi^3 N}(k_1k_2k_3k_4)^2 K\mathcal{T}_{\Phi,0}(k_1,k_2,k_3,k_4;K) = S_{\mathcal{T}}(k_1,k_2,k_3,k_4,K) = 1 \tag{64}$$

with N the normalization factor of Eq. (64) and the choice Δ_Φ^3 motivated by comparison to the local model. Again, as for the local model, the primordial trispectrum is already a zero mode quantity with respect to angle θ_4, i.e. $T = T_{,0}$. Using the Sachs-Wolfe approximation the integral (22) can be written as

$$\mathcal{T}^{l_1 l_2 \text{const}}_{l_3 l_4}(L) = \frac{\Delta_\Phi^3 N}{3^4}\left(\frac{2}{\pi}\right)^5 h_{l_1 l_2 L} h_{l_3 l_4 L} \times \int dx x^2 dr_1 r_1^3 I_{l_1}(0,r_1) I_{l_2}(0,r_1) \times I_{l_3}(0,r_1 x) I_{l_4}(0,r_1 x) I_L(1,x), \tag{65}$$

where we write $r_2/r_1 = x$. Now we can evaluate

$$I_l(0,x) = \frac{\pi}{2(2l+1)} x^{-(l+1)} \quad \text{for } x > 1 \qquad = \frac{\pi}{2(2l+1)} x^l \quad \text{for } x < 1, \tag{66}$$

$$I_L(1,x) = \frac{\pi\Gamma(L+1)}{2\Gamma(L+3/2)} x_2^{-(L+2)} F_1\left(\frac{1}{2}, L+1; L+\frac{3}{2}; x^{-2}\right) \quad \text{for } x > 1 \qquad = \frac{\pi\Gamma(L+1)}{2\Gamma(L+3/2)} x_2^{L} F_1\left(\frac{1}{2}, L+1; L+\frac{3}{2}; x^{2}\right) \quad \text{for } x < 1, \tag{67}$$

where ${}_2F_1$ is a generalized hypergeometric function. We can write ${}_2F_1$ in terms of a series expansion in the form

$${}_2F_1(a,b;c;z) = \sum_{n=0}^{\infty} \frac{(a)_n (b)_n}{(c)_n} \frac{z^n}{n!}, \tag{68}$$

where $(p)_n = \Gamma(p+n)/\Gamma(p)$. The conditions for convergence—namely, that this series converges for c a non-negative integer with $|z| < 1$—are satisfied in this case. Using this decomposition we find

$$\mathcal{T}^{l_1 l_2 \text{const}}_{l_3 l_4}(L) = \frac{\Delta_\Phi^3 N}{3^4} h_{l_1 l_2 L} h_{l_3 l_4 L} \frac{1}{\pi} \frac{1}{(2l_1+1)(2l_2+1)(2l_3+1)(2l_4+1)} \sum_{n=0}^{\infty} \frac{\Gamma(1/2+n)\Gamma(L+1+n)}{\Gamma(L+3/2+n)} \frac{1}{n!} \times \left[\frac{1}{2n+3+l_3+l_4+L}\left(\frac{1}{\sum l_i + 4} - \frac{1}{A_1}\right) + \frac{1}{2n+1+l_1+l_2+L}\left(\frac{1}{\sum l_i} + \frac{1}{A_1}\right) + \frac{1}{2n+3+l_1+l_2+L}\left(\frac{1}{\sum l_i + 4} - \frac{1}{A_2}\right) + \frac{1}{2n+1+l_3+l_4+L}\left(\frac{1}{\sum l_i} + \frac{1}{A_2}\right)\right]. \tag{69}$$

Notice that this sum is still finite if the denominators $A_1 = l_1 + l_2 - l_3 - l_4 + 2$ or $A_2 = l_3 + l_4 - l_1 - l_2 + 2$ are zero since in those cases the respective numerators vanish. Alternatively, we can integrate over the hypergeometric function directly and write the solution in the following closed form:

$$\mathcal{T}^{l_1 l_2 \text{const}}_{l_3 l_4}(L) = \frac{\Delta_\Phi^3 N}{3^4} h_{l_1 l_2 L} h_{l_3 l_4 L} \frac{1}{2\pi} \frac{1}{(2l_1+1)(2l_2+1)(2l_3+1)(2l_4+1)} B(L+1,1/2) \times \left[\left(\frac{1}{\sum l_i + 4} - \frac{1}{A_1}\right) B\left(\frac{C_1+2}{2},1\right) {}_3F_2\left(\left\{\frac{C_1+2}{2}, \frac{1}{2}, L+1\right\}; \left\{L+\frac{3}{2}, \frac{C_1+4}{2}\right\}; 1\right) + \left(\frac{1}{\sum l_i} + \frac{1}{A_1}\right) B\left(\frac{C_2}{2},1\right) {}_3F_2\left(\left\{\frac{C_2}{2}, \frac{1}{2}, L+1\right\}; \left\{L+\frac{3}{2}, \frac{C_2+2}{2}\right\}; 1\right) + \left(\frac{1}{\sum l_i + 4} - \frac{1}{A_2}\right) B\left(\frac{C_2+2}{2},1\right) {}_3F_2\left(\left\{\frac{C_2+2}{2}, \frac{1}{2}, L+1\right\}; \left\{L+\frac{3}{2}, \frac{C_2+4}{2}\right\}; 1\right) + \left(\frac{1}{\sum l_i} + \frac{1}{A_2}\right) B\left(\frac{C_1}{2},1\right) {}_3F_2\left(\left\{\frac{C_1}{2}, \frac{1}{2}, L+1\right\}; \left\{L+\frac{3}{2}, \frac{C_1+2}{2}\right\}; 1\right)\right], \tag{70}$$

where $B(x,y)$ denotes the beta function and $C_1 = 1 + l_3 + l_4 + L$, $C_2 = 1 + l_1 + l_2 + L$.

The equilateral shape has also received a lot of attention in the literature. As has been described in [14], for the purposes of data analyses, there are two representative forms for the equilateral trispectra. These are given by the following shapes for the reduced trispectra:

$$S^{\text{equil}}_{\mathcal{T},c_1}(\mathbf{k}_1, \mathbf{k}_2, \mathbf{k}_3, \mathbf{k}_4; \mathbf{K}) \propto K \frac{k_1 k_2 k_3 k_4}{(k_1 + k_2 + k_3 + k_4)^5}, \tag{71}$$

$$S^{\text{equil}}_{\mathcal{T},s_1}(\mathbf{k}_1, \mathbf{k}_2, \mathbf{k}_3, \mathbf{k}_4; \mathbf{K}) \propto \frac{k_1 k_2 k_3 k_4 K^2}{(k_3 + k_4 + K)^3} \left(\frac{1}{2(k_1 + k_2 + K)^3} + \frac{6(k_3 + k_4 + K)^2}{(k_1 + k_2 + k_3 + k_4)^5} + \frac{3(k_3 + k_4 + K)}{(k_1 + k_2 + k_3 + k_4)^4} + \frac{1}{(k_1 + k_2 + k_3 + k_4)^3} \right), \tag{72}$$

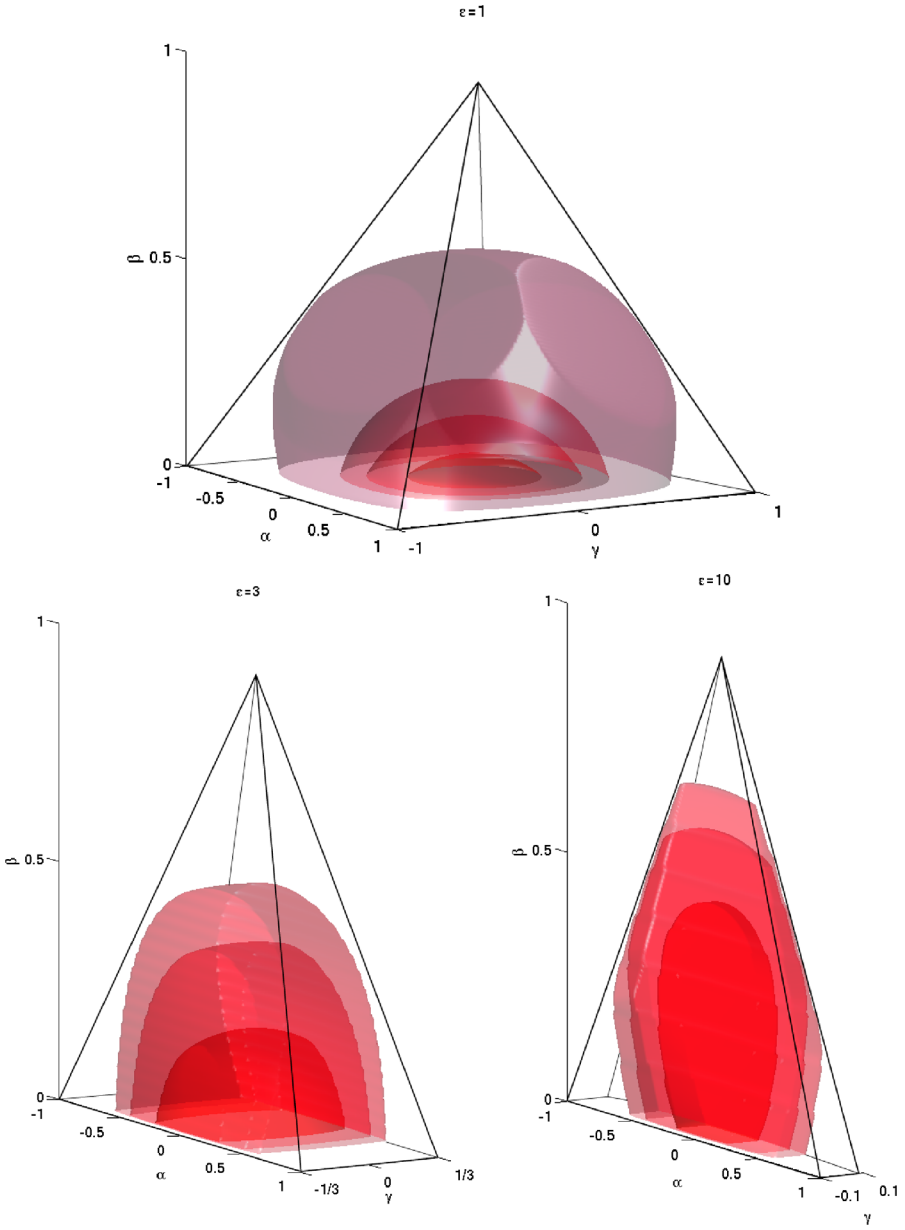

FIG. 6 (color online). Equilateral c_1 model (71). The signal peaks at $\epsilon = 1$ towards $\gamma = 0$, $\alpha = 0$, $\beta = 0$, i.e. at $k_1 = k_2 = k_3 = k_4 = K/2$. For $\epsilon > 1$ the signal similarly peaks for $k_1 = k_2$, $k_3 = k_4$, but since the triangles (k_1, k_2, K) and (k_3, k_4, K) are now unequal, the peak position is less sharp and shifts to smaller values of K.

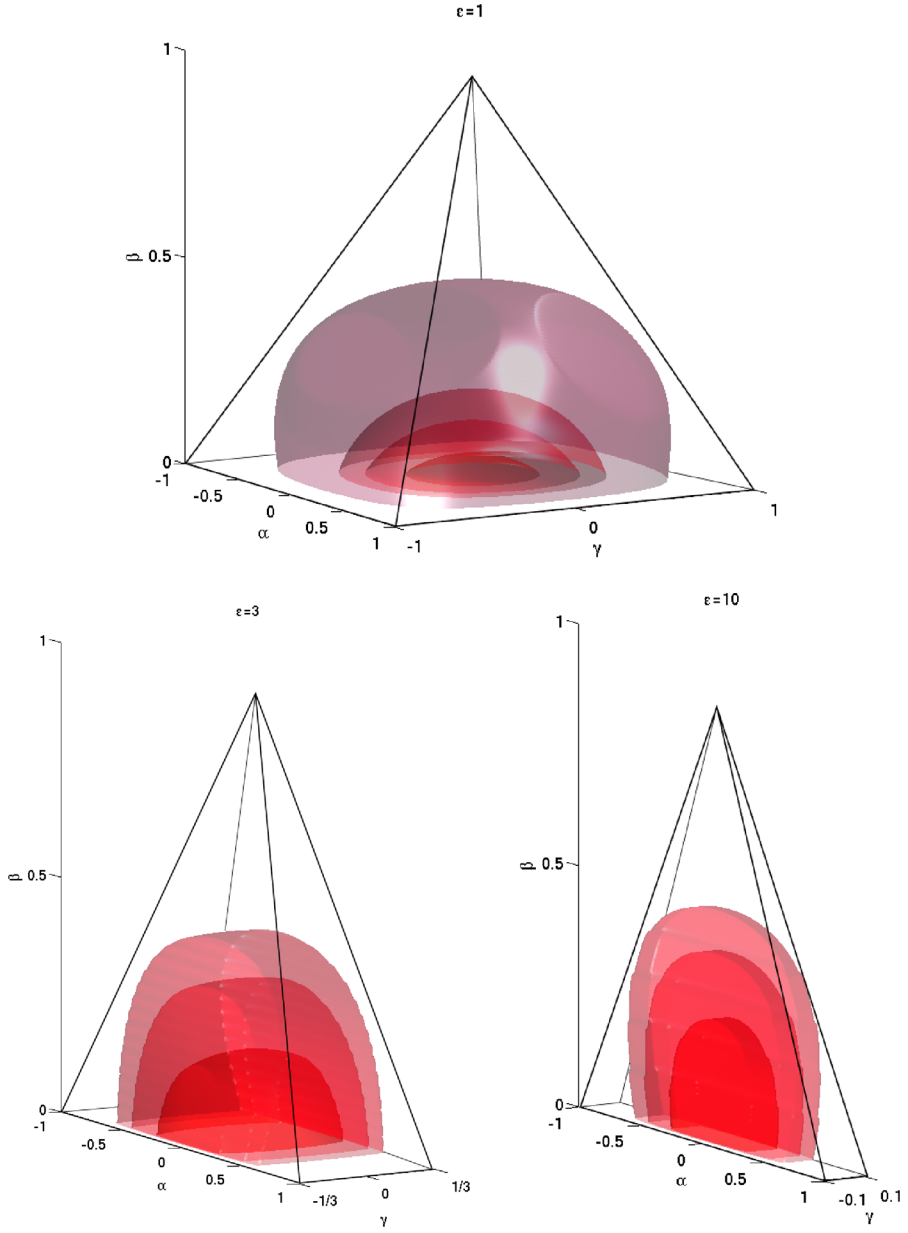

FIG. 7 (color online). Equilateral s_1 model (72). As for the equilateral c_1 model the signal peaks for equal k_i at ϵ, while for $\epsilon > 1$ the peak position becomes less sharp. As is clearly observable from the figures the equilateral c_1 and s_1 models are highly correlated.

where we use the notation c_1 and s_1 to correspond to [14]. These shapes are similar in most regions, apart from the doubly squeezed limit ($k_3 = k_4 \rightarrow 0$). It has been observed that the first ansatz is factorizable by introducing the integral $1/M^n = (1/\Gamma(n)) \int_0^\infty t^{n-1} e^{-Mt} dt$, where $M = \sum k_i$. As we observe from Figs. 6 and 7 it is clear that the shapes for the two representative forms are highly correlated. Therefore, for the purposes of the analysis of the equilateral model, it may only be necessary to consider the c_1 model.

V. MODE DECOMPOSITION

Our goal is to represent an arbitrary nonseparable reduced primordial trispectrum (zero mode) $\mathcal{T}_{\Phi,0}(k_1, k_2, k_3, k_4; K)$ or a reduced CMB trispectrum $\mathcal{T}^{l_1 l_2}_{l_3 l_4}(L)$ on their respective wave number or multipole domains using a rapidly convergent mode expansion. We need to achieve this in a separable manner, in order to make tractable the five-dimensional integrals ($\sim dk_1 dk_2 dk_3 dk_4 dK$) required for trispectrum estimation by breaking them down into products of one-dimensional integrals. In particular, this means that we wish to expand an arbitrary nonseparable primordial (reduced) shape function in the form

$$S_{\mathcal{T}}(k_1, k_2, k_3, k_4, K) = \sum_{p,r,s,u,v} \alpha_{prsuv} q_p(k_1) q_r(k_2) q_s(k_3) \times q_u(k_4) r_v(K), \quad (73)$$

where the q_p, r_v are appropriate basis mode functions which are convergent and complete; that is, they span the space of all functions on the wave number domain. The differing notation, q, r, is due to the different ranges of the variables—$k_i \in [0, k_{\rm max}]$ but $K \in [0, 2k_{\rm max}]$. In the case of more general probes of non-Gaussianity this is easily extended to include the other Legendre modes of Eq. (21) by writing

$$S(k_1, k_2, k_3, k_4, K, \theta_4) = \sum_n S_{\mathcal{T}n}(k_1, k_2, k_3, k_4, K) P_n(\cos\theta_4), \tag{74}$$

where S is the shape function applied to the full Legendre expansion (21). The shape function of the nth Legendre mode, $S_{\mathcal{T}n}$, may be decomposed as in Eq. (73).

We will present one method for finding the basis functions q, r below. We will achieve this objective in stages. First, we create examples of one-dimensional mode functions which are orthogonal and well behaved over the full wave number (or multipole) domain. We then construct five-dimensional products of these wave functions, $q_p(k_1)q_r(k_2)q_s(k_3)q_u(k_4)r_v(K) \to \mathcal{Q}_m$. This creates a complete basis for all possible reduced trispectra on the given domain. By orthonormalizing these product basis functions, $\mathcal{Q}_m \to \mathcal{R}_m$, we obtain a rapid and convenient method for calculating the expansion coefficients α_{prsuv} (or α_m). Here we use bounded symmetric polynomials as a concrete implementation of this methodology. Of course, as outlined in the case of the bispectrum in [1], there are alternatives to using the polynomials $\mathcal{Q}_m$, $\mathcal{R}_m$, but the shortcoming of these alternatives is that either (i) they can lead to overshooting at the domain boundaries or (ii) the choice may compromise separability. However, it is possible that an alternative to the polynomial expansion may be desirable to improve the rate of convergence. This should be able to conveniently represent functions in a separable form, and should be derived explicitly for the domain.

A. Domain and weight functions

In Fourier space, the primordial reduced trispectrum zero mode $\mathcal{T}_{\Phi,0}(k_1, k_2, k_3, k_4; K)$ is defined when the wave vectors $\mathbf{k_1}$, $\mathbf{k_2}$, $\mathbf{K}$ and $\mathbf{k_3}$, $\mathbf{k_4}$, $\mathbf{K}$ close to form triangles subject to $\mathbf{k_1} + \mathbf{k_2} + \mathbf{K} = 0 = \mathbf{k_3} + \mathbf{k_4} - \mathbf{K}$. Each such triangle is uniquely defined by the lengths of the sides k_1, k_2, K and k_3, k_4, K. In terms of these wave numbers, the triangle conditions restrict the allowed combinations into a region defined by

$$\begin{aligned} &k_1 \le K + k_2 \quad \text{for } k_1 \ge k_2, K, \quad \text{or} \quad k_2 \le K + k_1 \\ &\text{for } k_2 \ge k_1, K, \quad \text{or} \quad K \le k_1 + k_2 \quad \text{for } K \ge k_1, k_2 \end{aligned} \tag{75}$$

and

$$\begin{aligned} &k_3 \le K + k_4 \quad \text{for } k_3 \ge k_4, K, \quad \text{or} \quad k_4 \le K + k_3 \\ &\text{for } k_4 \ge k_3, K, \quad \text{or} \quad K \le k_3 + k_4 \quad \text{for } K \ge k_3, k_4. \end{aligned} \tag{76}$$

Since the wave number K is common to both triangles, the region is a product of the tetrahedral domains defined by the conditions (75) and (76). Considering each region individually we note that they each describe a regular tetrahedron for $k_1 + k_2 + K < 2k_{\rm max}$ (or $k_3 + k_4 + K < 2k_{\rm max}$). However, motivated by issues of separability and observation, it is more natural to extend the domain out to values given by a maximum wave number $k_{\rm max}$. In particular, we have $k_i < k_{\rm max}$ and $K < 2k_{\rm max}$. In each case the allowed region is a hexahedron formed by the intersection of a tetrahedron and a rectangular parallelepiped. For brevity we will denote this configuration as a tetrapiped. This region is an extension of the tetrapyd referred to in [1] due to the extended range of K, and is shown in Fig. 8.

In order to integrate functions $f(k_1, k_2, k_3, k_4, K)$ over the tetrapiped domains, which we denote $\mathcal{V}_{\mathcal{T}}$, we note the presence of K in both regions. We find that the integration is given explicitly by

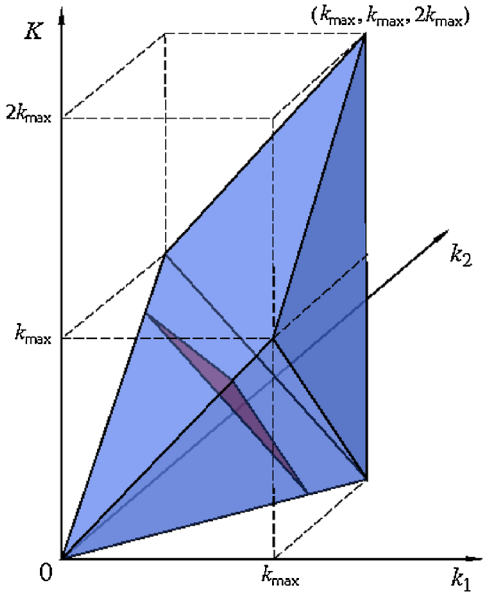

FIG. 8 (color online). "Tetrapiped" domain for allowed wave numbers of the primordial reduced trispectrum $\mathcal{T}(k_1, k_2, k_3, k_4; K, \theta_4)$ imposed by the triangle created by (k_1, k_2, K). There is a corresponding tetrapiped domain imposed by the triangle created by (k_3, k_4, K). The region is an extension of the tetrapyd domain described in [1] due to the extended range of K. The same domain is valid for allowed multipole values l_i, L in the case of the reduced CMB trispectrum $\mathcal{T}^{l_1 l_2}_{l_3 l_4}(L)$. The shaded area denotes the region described in Fig. 3.

$$\mathcal{I}[f] \equiv \int_{\mathcal{V}_\mathcal{T}} f(k_1, k_2, k_3, k_4, K)\omega(k_1, k_2, k_3, k_4, K)d\mathcal{V}_\mathcal{T}$$
$$= k_{\rm max}^5\Bigg\{\int_0^{1/2} dt\Bigg(\int_0^t ds\int_{t-s}^{t+s} dx + \int_t^{1-t} ds\int_{s-t}^{t+s} dx + \int_{1-t}^1 ds\int_{s-t}^1 dx\Bigg)$$
$$\times\Bigg(\int_0^t dy\int_{t-y}^{t+y} dz + \int_t^{1-t} dy\int_{y-t}^{t+y} dz + \int_{1-t}^1 dy\int_{y-t}^1 dz\Bigg)FW$$
$$+\int_{1/2}^1 dtFW\Bigg(\int_0^{1-t} ds\int_{t-s}^{t+s} dx + \int_{1-t}^t ds\int_{t-s}^{t+s} dx + \int_t^1 ds\int_{s-t}^1 dx\Bigg)$$
$$\times\Bigg(\int_0^{1-t} dy\int_{t-y}^{t+y} dz + \int_{1-t}^t dy\int_{t-y}^{t+y} dz + \int_t^1 dy\int_{y-t}^1 dz\Bigg) + \int_1^2 dt\int_{t-1}^1 ds\int_{t-s}^1 dx\int_{t-1}^1 dy\int_{t-y}^1 dzFW\Bigg\}, \quad (77)$$

where $\omega(k_1, k_2, k_3, k_4, K)$ is an appropriate weight function and we have made the transformation $t = K/k_{\rm max}$, $s = k_1/k_{\rm max}$, $x = k_2/k_{\rm max}$, $y = k_3/k_{\rm max}$, $z = k_4/k_{\rm max}$ with $F(s, x, y, z, t) = f(k_{\rm max} \times (s, x, y, z, t))$ and $W(s, x, y, z, t) = \omega(k_{\rm max} \times (s, x, y, z, t))$. For integrals over the product of two functions f and g, we can define the inner product $\langle f, g\rangle = \mathcal{I}[fg]$. This inner product essentially defines a Hilbert space of possible shape functions in the domain. The total volume of the domain is given by $\mathcal{I}[1] = k_{\rm max}^5/3$. Initially we will restrict our attention to the case of weight $\omega = 1$. However, it is important to incorporate a weight function for a variety of reasons which we will discuss later.

Analysis of the CMB extra-reduced trispectrum $t^{l_1l_2}_{l_3l_4}(L)$ is more straightforward than in the primordial case. This is because the CMB trispectrum, being defined on a two-sphere, is an explicitly five-dimensional quantity and therefore is defined completely in terms of the multipoles. We note here that the quantity $p^{l_1l_2}_{l_3l_4}(L) = t^{l_1l_2}_{l_3l_4}(L) + t^{l_2l_1}_{l_3l_4}(L) + t^{l_1l_2}_{l_4l_3}(L) + t^{l_2l_1}_{l_4l_3}(L)$ is probably a more elegant expression for this analysis since it is more symmetric while being defined on the same domain and being subject to the same weighting over the domain. Nonetheless, we proceed in this paper with the analysis of $t^{l_1l_2}_{l_3l_4}(L)$, leaving exploration of this minor issue to an upcoming paper [40]. As for the primordial case, we extend the tetrahedral domains to include multipoles out to l_i, $L/2 < l_{\rm max}$. The respective tetrapiped domains for the extra-reduced trispectrum become the discrete $\{l_1, l_2, l_3, l_4, L\}$ satisfying

$$l_1, l_2, l_3, l_4, L/2 < l_{\rm max}, l_i, L \in \mathbb{N},$$
$$l_1 \le l_2 + L \quad \text{for } l_1 \ge l_1, L, +\text{cyclic perms},$$
$$l_3 \le l_4 + L \quad \text{for } l_3 \ge l_4, L, +\text{cyclic perms},$$
$$l_1 + l_2 + L = 2n_1, \qquad l_3 + l_4 + L = 2n_2,$$
$$n_1, n_2 \in \mathbb{N}. \quad (78)$$

In multipole space, we will be primarily dealing with a summation over all possible $\{l_1, l_2, l_3, l_4, L\}$ combinations in the correlator $\mathcal{C}(\mathcal{T}, \mathcal{T}')$. The appropriate weight function in the sum from (23) is then

$$\omega(l_1, l_2, l_3, l_4, L) = h^2_{l_1l_2L}h^2_{l_3l_4L}. \quad (79)$$

A straightforward continuum version of this can be deduced by comparison of this "weight" formula to the bispectrum multipole weight function in [1]. Similarly to that analysis, we should eliminate a scaling in this weight such that the overall weight becomes very nearly constant. We can do this by using a separable weight function as

$$\omega_s(l_1l_2l_3l_4L) = \frac{\omega(l_1, l_2, l_3, l_4, L)}{(2l_1 + 1)^{1/3}(2l_2 + 1)^{1/3}(2l_3 + 1)^{1/3}(2l_4 + 1)^{1/3}(2L + 1)^{2/3}}. \quad (80)$$

We note that there is also a freedom to absorb an arbitrary separable function υ_l into the weight functions. If we define a new weight $\bar{\omega}$ in the estimator as

$$\bar{\omega}_{\,l_1l_2l_3l_4L} = \omega_{l_1l_2l_3l_4L}/(\upsilon_{l_1}\upsilon_{l_2}\upsilon_{l_3}\upsilon_{l_4}\upsilon_L)^2, \quad (81)$$

then we must rescale the estimator functions by the factor $\upsilon_{l_1}\upsilon_{l_2}\upsilon_{l_3}\upsilon_{l_4}\upsilon_L$. The important point is to use both the weight $\bar{\omega}$ and the estimator rescaling throughout the analysis, including the generation of appropriate orthonormal mode functions.

B. Orthogonal polynomials on the domain

We now construct some concrete realizations of mode functions which are orthogonal on the domain $\mathcal{V}_\mathcal{T}$ and which have the form required for a separable expansion. First, we will generate one-dimensional orthogonal polynomials $q_p(s)$, $r_v(t)$ for unit weight $\omega = 1$. Considering functions $q_p(s)$ depending only on the s coordinate,[3] we integrate over the t, x, y, z directions to yield the weight

[3]We can consider s as corresponding to any of the k_i.

functions $\bar{\omega}(s)$ for $s \in [0, 1]$ (for simplicity, we take $k_{\max} = 1$):

$$\bar{\omega}(s) = s - s^3 + \frac{5}{12}s^4, \quad \text{with} \quad \mathcal{I}[f] = \int_0^1 f(s)\bar{\omega}(s)\text{ds}. \tag{82}$$

Therefore, the moments for each power of s become

$$\bar{\omega}_n \equiv \mathcal{I}[s^n] = \frac{1}{n+2} + \frac{5}{12(n+5)} - \frac{1}{n+4} = \frac{5n^2 + 54n + 160}{12(n+2)(n+4)(n+5)}. \tag{83}$$

For functions $r_v(t)$ (where t corresponds to the K coordinate), we integrate over the s, x, y, z directions to yield the weight functions $\hat{\omega}(t)$ for $t \in [0, 2]$:

$$\hat{\omega}(t) = \left(\frac{t}{2}(4 - 3t)\right)^2 \quad \text{for } t \in [0, 1] = \frac{(t-2)^4}{4} \quad \text{for } t \in [1, 2], \quad \text{with} \quad \mathcal{I}[f] = \int_0^2 f(t)\hat{\omega}(t)dt. \tag{84}$$

With this choice of weight the moments of each power of t become

$$\hat{\omega}_n \equiv \mathcal{I}[t^n] = \frac{n^2 + 15n + 68}{4(n+3)(n+4)(n+5)} + \frac{768 \times 2^n - 744 - 474n - 131n^2 - 18n^3 - n^4}{4(n+1)(n+2)(n+3)(n+4)(n+5)}. \tag{85}$$

From these moments we can create orthogonal polynomials using the generating functions,

$$q_n(s) = \frac{1}{\mathcal{N}_1}\begin{vmatrix} 1/3 & 73/360 & 1/7 & \dots & \bar{\omega}_n \\ 73/360 & 1/7 & 367/3360 & \dots & \bar{\omega}_{n+1} \\ \dots & \dots & \dots & \dots & \dots \\ \bar{\omega}_{n-1} & \bar{\omega}_n & \bar{\omega}_{n+1} & \dots & \bar{\omega}_{2n-1} \\ 1 & s & s^2 & \dots & s^n \end{vmatrix} \tag{86}$$

and

$$r_n(t) = \frac{1}{\mathcal{N}_2}\begin{vmatrix} 1/3 & 7/30 & 4/21 & \dots & \hat{\omega}_n \\ 7/30 & 4/21 & 73/420 & \dots & \hat{\omega}_{n+1} \\ \dots & \dots & \dots & \dots & \dots \\ \hat{\omega}_{n-1} & \hat{\omega}_n & \hat{\omega}_{n+1} & \dots & \hat{\omega}_{2n-1} \\ 1 & t & t^2 & \dots & t^n \end{vmatrix}, \tag{87}$$

where we choose the normalization factors $\mathcal{N}_1$, $\mathcal{N}_2$ such that $\mathcal{I}[q_n^2] = 1$ and $\mathcal{I}[r_n^2] = 1$ for all $n \in \mathbb{N}$, that is, such that the $q_n(s)$ [or $r_n(t)$] are orthonormal,

$$\langle q_n, q_p \rangle \equiv \mathcal{I}[q_n q_p] = \int_{\mathcal{V}_\mathcal{T}} q_n(s)q_p(s)d\mathcal{V}_\mathcal{T} = \delta_{np}, \tag{88}$$

$$\langle r_v, r_u \rangle \equiv \mathcal{I}[r_v r_u] = \int_{\mathcal{V}_\mathcal{T}} r_v(t)r_v(t)d\mathcal{V}_\mathcal{T} = \delta_{vu}. \tag{89}$$

The first few orthonormal polynomials on the domain $\mathcal{V}_\mathcal{T}$ are explicitly

$$\begin{aligned} q_0(s) &= \sqrt{3}, \\ q_1(s) &= 7.161\,03(-0.608\,333 + s), \\ q_2(s) &= 7.767\,59 - 33.2061s + 29.0098s^2, \\ q_3(s) &= -11.7911 + 93.1318s - 194.111s^2 + 116.964s^3, \dots \end{aligned} \tag{90}$$

and

$$
\begin{aligned}
r_0(t) &= \sqrt{3}, \\
r_1(t) &= 6.069\,77(-0.7 + t), \\
r_2(t) &= 7.650\,66 - 24.1493t + 16.1942t^2, \\
r_3(t) &= -12.2182 + 63.4315t - 91.6438t^2 \\
&\quad + 38.7091t^3, \ldots .
\end{aligned} \tag{91}
$$

We note that the q_n's and r_v's are only orthogonal in one dimension [e.g. $\langle q_n(s) r_v(t)\rangle \neq \delta_{nv}$ and $\langle q_n(s) q_m(x)\rangle \neq \delta_{nm}$]. However, as product functions of t, s, x, y, and z, they form an independent and well-behaved basis which we will use to construct orthonormal five-dimensional eigenfunctions. In practice, the q_n's and r_v's remain the primary calculation tools, notably in performing separable integrations. In Fig. 9 we plot the first few q_n's and r_v's.

Now we turn to the polynomials $\bar{\mathcal{Q}}(s)$ and $\bar{\mathcal{R}}(t)$, which are orthonormal on the multipole domain. Using the weight function $\omega = 1$ we find the same polynomials as above. For the scaled weight function ω_s the polynomials will, of course, differ. While either polynomial set would suffice as independent basis functions on the multipole domain, the use of correctly weighted functions leads to improvements in the immediate orthogonality of the derived five-dimensional polynomial sets. For definiteness we take $(t, s, x, y, z) \times l_{\max} = (L, l_1, l_2, l_3, l_4)$. The generating function is obtained as above but now using the moments $\bar{\omega}_n \equiv \mathcal{I}[s^n] = \int \omega(t, s, x, y, z) s^n d\mathcal{V}_{\mathcal{T}}$ and $\hat{\omega}_n \equiv \mathcal{I}[t^n] = \int \omega(t, s, x, y, z) t^n d\mathcal{V}_{\mathcal{T}}$.

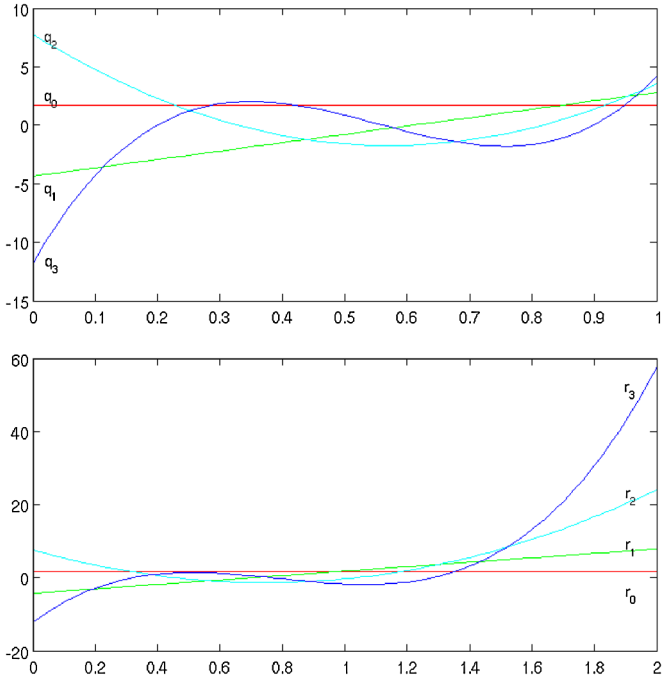

FIG. 9 (color online). The orthonormal one-dimensional eigenmodes q_n, r_v plotted on their respective domains for $n, v = 0, 1, 2, 3$. The q_n, r_v plotted are calculated for unit weight $\omega = 1$ on the domain $\mathcal{V}_{\mathcal{T}}$. The shape of these eigenmodes alters for different choices of the weighting.

C. Five-dimensional basis functions

We can represent arbitrary (reduced) trispectra Legendre modes on the domain $\mathcal{V}_{\mathcal{T}}$ using a suitable set of independent basis functions formed from products $q_p(s) q_r(x) q_s(y) q_u(z) r_v(t)$. (Here again we take $t = K/k_{\max}$, $s = k_1/k_{\max}$, $x = k_2/k_{\max}$, $y = k_3/k_{\max}$, $z = k_4/k_{\max}$, or $t = L/l_{\max}$, etc.) We denote the 5D basis function as

$$
\mathcal{Q}_m(t, s, x, y, z) = q_p(s) q_r(x) q_s(y) q_u(z) r_v(t). \tag{92}
$$

We can order these products linearly with a single index m in a similar manner to that described in [1] for the bispectrum.

While the $\mathcal{Q}_m$'s by construction are an independent set of five-dimensional functions on the domain $\mathcal{V}_{\mathcal{T}}$, they are not, in general, orthogonal. To construct an orthonormal set $\mathcal{R}_m$ from the $\mathcal{Q}_m$ we perform an iterative Gram-Schmidt orthogonalization process such that

$$
\langle \mathcal{R}_n \mathcal{R}_m \rangle = \delta_{nm}. \tag{93}
$$

In particular, we form the Gram matrix $\Gamma = (\langle \mathcal{Q}_n \mathcal{Q}_m \rangle)$ which needs to be factorized as $\Gamma = \Lambda^T \Lambda$ where $\Lambda = (\langle \mathcal{Q}_n \mathcal{R}_m \rangle)$ is triangular. This process is described in more detail in [1].

D. Mode decomposition of the trispectrum

Having formed the orthonormal basis $\{\mathcal{R}_m\}$ we consider an arbitrary primordial reduced trispectrum (zero mode) $\mathcal{T}_{,0}(k_1, k_2, k_3, k_4; K)$ described by the shape function $S_{\mathcal{T}}$ and decompose it as follows:

$$
S_{\mathcal{T}}(k_1, k_2, k_3, k_4, K) = \sum_m \alpha_m^{\mathcal{R}} \mathcal{R}_m(t, s, x, y, z), \tag{94}
$$

where the expansion coefficients $\alpha_m^{\mathcal{R}}$ are given by

$$
\alpha_m^{\mathcal{R}} = \langle \mathcal{R}_m, S_{\mathcal{T}} \rangle = \int_{\mathcal{V}_{\mathcal{T}}} \mathcal{R}_m S_{\mathcal{T}} \omega d\mathcal{V}_{\mathcal{T}} \tag{95}
$$

and $k_{\max}(t, s, x, y, z) = (K, k_1, k_2, k_3, k_4)$ on the domain $\mathcal{V}_{\mathcal{T}}$ defined in (75) and (76). In practice, we must always work with partial sums up to a given $N = n_{\max}$ with

$$
S_{\mathcal{T}}^N = \sum_{m=0}^{N} \alpha_m^{\mathcal{R}} \mathcal{R}_m(t, s, x, y, z), \qquad S_{\mathcal{T}} = \lim_{N\to\infty} S_{\mathcal{T}}^N. \tag{96}
$$

Given the complete orthonormal basis $\mathcal{R}_m$, Parseval's theorem for the integrated product of two functions implies

$$
\langle S_{\mathcal{T}}, S'_{\mathcal{T}} \rangle = \int_{\mathcal{V}_{\mathcal{T}}} S_{\mathcal{T}} S'_{\mathcal{T}} \omega d\mathcal{V}_{\mathcal{T}} = \lim_{N\to\infty} \sum_{m=0}^{N} \alpha_m^{\mathcal{R}} \alpha_m^{\mathcal{R}'}, \tag{97}
$$

which for the square of a mode $S_{\mathcal{I}}$ yields the sum of the squares of the expansion coefficients, $\mathcal{I}[S^2_{\mathcal{I}}] = \sum_m \alpha^{\mathcal{R}2}_m$.

In order to accomplish the goal of a general separable expansion, we must transform backwards from the orthogonal sum $\mathcal{R}_m$ into an expansion over the separable product functions $\mathcal{Q}_m$ through

$$S^N_{\mathcal{I}} = \sum_{m=0}^{N} \alpha^{\mathcal{Q}}_m \mathcal{Q}_m(t, s, x, y, z). \tag{98}$$

The $\alpha^{\mathcal{Q}}_m$ can be obtained from the $\alpha^{\mathcal{R}}_m$ via

$$\alpha^{\mathcal{Q}}_m = \sum_{p=0}^{N} (\lambda^T)_{mp} \alpha^{\mathcal{R}}_p, \tag{99}$$

where the transformation matrix λ_{np} was defined above. Using the inverse relation $\alpha^{\mathcal{R}}_m = \sum_{p=0}^{N} (\lambda^T)^{-1}_{mp} \alpha^{\mathcal{Q}}_p$ we find that the matrices Γ and Λ are related by

$$(\gamma^{-1})_{np} = \sum_{r}^{N} (\lambda^T)_{nr} \lambda_{rp}. \tag{100}$$

This implies that

$$\langle S^N_{\mathcal{I}}, S^N_{\mathcal{I}} \rangle = \sum_{m=0}^{N} \alpha^{\mathcal{R}2}_m = \sum_{m=0}^{N} \sum_{p=0}^{N} \alpha^{\mathcal{Q}}_m \gamma_{mp} \alpha^{\mathcal{Q}}_p. \tag{101}$$

As we have already noted, the separable $\mathcal{Q}_m$ expansion is most useful for practical calculations. However, its coefficients must be constructed from the orthonormal $\mathcal{R}_m$.

We can expand the CMB extra-reduced trispectrum $t^{l_1 l_2}_{l_3 l_4}(L)$ at late times using the same polynomials. However, as noted previously the CMB trispectrum is an explicitly five-dimensional quantity and, as such, we do not require the extra step of finding the zero mode of the Legendre series expansion. In particular, the appropriate expansion is of the form $t^{l_1 l_2}_{l_3 l_4}(L) = \sum_m \bar{\alpha}^{\mathcal{R}}_m \mathcal{R}_m(t, s, x, y, z) (= \sum_m \bar{\alpha}^{\mathcal{Q}}_m \mathcal{Q}_m(t, s, x, y, z))$.

VI. MEASURES OF T_{NL}

A. Primordial estimator

We have obtained related mode expansions for a general primordial shape function, one with the orthonormal basis $\mathcal{R}_m$ and the other with the separable basis functions $\mathcal{Q}_m$. Substitution of the (reduced) separable form into the expression for the extra-reduced trispectrum (23) offers an efficient route to its direct calculation through

$$\begin{aligned} t^{l_1 l_2}_{l_3 l_4}(L) &= N \Delta^3_\Phi \left(\frac{2}{\pi}\right)^5 \int r_1^2 dr_1 r_2^2 dr_2 dk_1 dk_2 dk_3 dk_4 dK K \sum_m \alpha^{\mathcal{Q}}_m \mathcal{Q}_m(k_1, k_2, k_3, k_4, K) j_L(Kr_1) j_L(Kr_2) [j_{l_1}(k_1 r_1) \Delta_{l_1}(k_1)] \\ &\quad \times [j_{l_2}(k_2 r_1) \Delta_{l_2}(k_2)] [j_{l_3}(k_3 r_2) \Delta_{l_3}(k_3)] [j_{l_4}(k_4 r_2) \Delta_{l_4}(k_4)] \\ &= N \Delta^3_\Phi \sum_m \alpha^{\mathcal{Q}}_m \int r_1^2 dr_1 r_2^2 dr_2 \mathcal{Q}^{l_1 l_2 l_3 l_4 L}_m(r_1, r_2), \end{aligned} \tag{102}$$

where

$$\mathcal{Q}^{l_1 l_2 l_3 l_4 L}_m(r_1, r_2) = q^{l_1}_p(r_1) q^{l_2}_r(r_1) q^{l_3}_s(r_2) q^{l_4}_u(r_2) r^L_v(r_1, r_2) \tag{103}$$

with

$$\begin{aligned} q^l_p(r) &= \frac{2}{\pi} \int dk q_p(k) \Delta_l(k) j_l(kr), \\ r^L_v(r_1, r_2) &= \frac{2}{\pi} \int dK K r_v(K) j_L(Kr_1) j_L(Kr_2). \end{aligned} \tag{104}$$

Next, we note from (11) that

$$\mathcal{T}_{l_1 m_1 l_2 m_2 l_3 m_3 l_4 m_4} = \sum_{LM} (-1)^M \begin{pmatrix} l_1 & l_2 & L \\ m_1 & m_2 & -M \end{pmatrix} \times \begin{pmatrix} l_3 & l_4 & L \\ m_3 & m_4 & M \end{pmatrix} \mathcal{T}^{l_1 l_2}_{l_3 l_4}(L). \tag{105}$$

Therefore, using these formulas in the estimator (28) (we omit the normalization factor N_T here and return to it later in the section) we find

$$\begin{aligned} \mathcal{E} &= 12 \sum_{l_i m_i} \mathcal{T}_{l_1 m_1 l_2 m_2 l_3 m_3 l_4 m_4} \frac{(a_{l_1 m_1} a_{l_2 m_2} a_{l_3 m_3} a_{l_4 m_4})_c}{C_{l_1} C_{l_2} C_{l_3} C_{l_4}} \Rightarrow \mathcal{E} \\ &= \sum_{l_i m_i} \sum_{LM} 12 N \Delta^3_\Phi \Big[\left(\int d\hat{n}_1 Y_{l_1 m_1}(\hat{n}_1) Y_{l_2 m_2}(\hat{n}_1) Y^*_{LM}(\hat{n}_1) \right) \\ &\quad \times \left(\int d\hat{n}_2 Y_{l_3 m_3}(\hat{n}_2) Y_{l_4 m_4}(\hat{n}_2) Y_{LM}(\hat{n}_2) \right) \sum_m \alpha^{\mathcal{Q}}_m \int r_1^2 dr_1 r_2^2 dr_2 \mathcal{Q}^{l_1 l_2 l_3 l_4 L}_m(r_1, r_2) \Big] \frac{(a_{l_1 m_1} a_{l_2 m_2} a_{l_3 m_3} a_{l_4 m_4})_c}{C_{l_1} C_{l_2} C_{l_3} C_{l_4}}. \end{aligned} \tag{106}$$

Now using the notation $\mathcal{E} = \mathcal{E}_{\rm tot} - \mathcal{E}_{\rm uc}$, where "tot" refers to $a_{l_1m_1}a_{l_2m_2}a_{l_3m_3}a_{l_4m_4}$ and "uc" refers to $(a_{l_1m_1}a_{l_2m_2}a_{l_3m_3}a_{l_4m_4})_{\rm uc}$, in place of $(a_{l_1m_1}a_{l_2m_2}a_{l_3m_3}a_{l_4m_4})_c$, we find

$$\mathcal{E}_{\rm uc} = 12N\Delta_\Phi^3 \sum_m \alpha_m^{\mathcal{Q}} \int d\hat{n}_1 d\hat{n}_2 \int dr_1 dr_2 r_1^2 r_2^2 N_v(\hat{n}_1, \hat{n}_2, r_1, r_2)(M_{pr}^{\rm uc}(\hat{n}_1, \hat{n}_1, r_1, r_1)M_{su}^{\rm uc}(\hat{n}_2, \hat{n}_2, r_2, r_2) + M_{ps}^{\rm uc}(\hat{n}_1, \hat{n}_2, r_1, r_2)M_{ru}^{\rm uc}(\hat{n}_1, \hat{n}_2, r_1, r_2) + M_{pu}^{\rm uc}(\hat{n}_1, \hat{n}_2, r_1, r_2)M_{rs}^{\rm uc}(\hat{n}_1, \hat{n}_2, r_1, r_2)) \quad (107)$$

and

$$\mathcal{E}_{\rm tot} = 12N\Delta_\Phi^3 \sum_m \alpha_m^{\mathcal{Q}} \int d\hat{n}_1 d\hat{n}_2 \int dr_1 dr_2 r_1^2 r_2^2 M_p(\hat{n}_1, r_1)M_r(\hat{n}_1, r_1)M_s(\hat{n}_2, r_2)M_u(\hat{n}_2, r_2)N_v(\hat{n}_1, \hat{n}_2, r_1, r_2), \quad (108)$$

where

$$M_{ps}^{\rm uc}(\hat{n}_1, \hat{n}_2, r_1, r_2) = \sum_{l_1m_1} \frac{Y_{l_1m_1}(\hat{n}_1)Y^*_{l_1m_1}(\hat{n}_2)q_p^{l_1}(r_1)q_s^{l_1}(r_2)}{C_{l_1}},$$
$$M_p(\hat{n}_1, r_1) = \sum_{l_1m_1} \frac{Y_{l_1m_1}(\hat{n}_1)a_{l_1m_1}q_p^{l_1}(r_1)}{C_{l_1}}, \quad (109)$$
$$N_v(\hat{n}_1, \hat{n}_2, r_1, r_2) = \sum_{LM} Y^*_{LM}(\hat{n}_1)Y_{LM}(\hat{n}_2)r_v^L(r_1, r_2).$$

We can summarize these results (substituting back in N_T) as

$$\mathcal{E} = \frac{12N\Delta_\Phi^3}{N_T} \sum_m \alpha_m^{\mathcal{Q}} \int d\hat{n}_1 d\hat{n}_2 \int dr_1 dr_2 r_1^2 r_2^2 \times \mathcal{M}_m^{\mathcal{Q}}(\hat{n}_1, \hat{n}_2, r_1, r_2) = \frac{N\Delta_\Phi^3}{N_T} \sum_m \alpha_m^{\mathcal{Q}} \beta_m^{\mathcal{Q}}, \quad (110)$$

with

$$\beta_m^{\mathcal{Q}} = 12 \int d\hat{n}_1 d\hat{n}_2 \int dr_1 dr_2 r_1^2 r_2^2 \mathcal{M}_m^{\mathcal{Q}}(\hat{n}_1, \hat{n}_2, r_1, r_2) \quad (111)$$

and the form of $\mathcal{M}_m^{\mathcal{Q}}$ inferred from the above equations. The estimator has been reduced entirely to tractable integrals and sums which can be performed relatively quickly.

We can estimate the computational time needed to find this estimator. The multipole summation needed for each basis is $\mathcal{O}(l_{\rm max})$ (since the sum over the m's can be precomputed). The integral $\sim \int d^2\hat{n}$ is an $\mathcal{O}(l_{\rm max}^2)$ calculation, while the line of sight integral $\sim \int dr$ is conservatively estimated as an $\mathcal{O}(100)$ operation. Therefore, in total the estimated number of operations is $\mathcal{O}(10\,000) \times \mathcal{O}(l_{\rm max}^5)$.

In the case that the primordial trispectrum is independent of the diagonal K, the estimated number of operations reduces to $\mathcal{O}(100) \times \mathcal{O}(l_{\rm max}^3)$ as outlined in Appendix D.

B. CMB estimator

In the case of a precomputed CMB trispectrum or a late-time source of non-Gaussianity in the CMB, such as gravitational lensing or active models such as cosmic strings, we wish to find a late-time CMB estimator. For the late-time analysis we wish to expand the estimator functions using the separable $\bar{\mathcal{Q}}_m(l_1, l_2, l_3, l_4, L)$ mode functions created out of the $\bar{\mathcal{Q}}_p(l)$ and $\bar{\mathcal{R}}_v(L)$ polynomials. (Note that we denote the multipole modes with a bar to distinguish them from the primordial equivalents, and also that we have no need for a subscript for the zeroth Legendre mode since the CMB trispectrum is an explicitly five-dimensional quantity as described earlier.) In order to effectively expand in mode functions modulated by the C_l's, we choose to decompose the estimator functions directly as

$$\frac{\upsilon_{l_1}\upsilon_{l_2}\upsilon_{l_3}\upsilon_{l_4}\upsilon_L}{\sqrt{C_{l_1}C_{l_2}C_{l_3}C_{l_4}}} t_{l_3l_4}^{l_1l_2}(L) = \sum_m \bar{\alpha}_m^{\mathcal{Q}} \bar{\mathcal{Q}}_m, \quad (112)$$

where the separable υ_l incorporates the freedom to make the weight function ω even more scale invariant. The estimator expansion with C_l in (106) is appropriate for primordial models, but it is expected that flatter choices will be more suitable for late-time anisotropy, such as from cosmic strings.

Substituting this mode expansion into the estimator (28) (where again we omit the normalization factor N_T and return to it later in the section), we find

$$\mathcal{E} = 12 \sum_{l_im_i} \sum_{LM} \sum_n \bar{\alpha}_n^{\mathcal{Q}} \bar{\mathcal{Q}}_p(l_1)\bar{\mathcal{Q}}_r(l_2)\bar{\mathcal{Q}}_s(l_3)\bar{\mathcal{Q}}_u(l_4)\bar{\mathcal{R}}_v(L) \times \int d^2\hat{n}_1 Y_{l_1m_1}(\hat{n}_1)Y_{l_2m_2}(\hat{n}_1)Y^*_{LM}(\hat{n}_1) \times \int d^2\hat{n}_2 Y_{l_3m_3}(\hat{n}_2)Y_{l_4m_4}(\hat{n}_2)Y_{LM}(\hat{n}_2) \times \frac{(a_{l_1m_1}a_{l_2m_2}a_{l_3m_3}a_{l_4m_4})_c}{\upsilon_{l_1}\upsilon_{l_2}\upsilon_{l_3}\upsilon_{l_4}\upsilon_L\sqrt{C_{l_1}C_{l_2}C_{l_3}C_{l_4}}}. \quad (113)$$

After some algebra we find

$$\mathcal{E}^{\rm tot} = 12N\Delta_\Phi^3 \sum_n \bar{\alpha}_n^{\mathcal{Q}} \int d^2\hat{n}_1 d^2\hat{n}_2 \bar{\mathcal{M}}_p(\hat{n}_1)\bar{\mathcal{M}}_r(\hat{n}_1)\bar{\mathcal{M}}_s(\hat{n}_2) \times \bar{\mathcal{M}}_u(\hat{n}_2)\bar{\mathcal{N}}_v(\hat{n}_1,\hat{n}_2),$$

$$\mathcal{E}^{\rm uc} = 12N\Delta_\Phi^3 \sum_n \bar{\alpha}_n^{\mathcal{Q}} \int d^2\hat{n}_1 d^2\hat{n}_2 (\bar{\mathcal{M}}^{\rm uc}_{pr}(\hat{n}_1,\hat{n}_1)\bar{\mathcal{M}}^{\rm uc}_{su}(\hat{n}_2,\hat{n}_2) + \bar{\mathcal{M}}^{\rm uc}_{ps}(\hat{n}_1,\hat{n}_2)\bar{\mathcal{M}}^{\rm uc}_{ru}(\hat{n}_1,\hat{n}_2) + \bar{\mathcal{M}}^{\rm uc}_{pu}(\hat{n}_1,\hat{n}_2)\bar{\mathcal{M}}^{\rm uc}_{rs}(\hat{n}_1,\hat{n}_2))\bar{\mathcal{N}}_v(\hat{n}_1,\hat{n}_2), \quad (114)$$

where

$$\bar{\mathcal{M}}_p(\hat{n}_1) = \sum_{l_1m_1} \frac{a_{l_1m_1}Y_{l_1m_1}(\hat{n}_1)\bar{\mathcal{Q}}_p(l_1)}{v_{l_1}\sqrt{C_{l_1}}},$$

$$\bar{\mathcal{M}}^{\rm uc}_{ps}(\hat{n}_1,\hat{n}_2) = \sum_{l_1m_1} \frac{Y_{l_1m_1}(\hat{n}_1)Y^*_{l_1m_1}(\hat{n}_2)\bar{\mathcal{Q}}_p(l_1)\bar{\mathcal{Q}}_s(l_1)}{v^2_{l_1}},$$

$$\bar{\mathcal{N}}_v(\hat{n}_1,\hat{n}_2) = \sum_{LM} \frac{Y^*_{LM}(\hat{n}_1)Y_{LM}(\hat{n}_2)\bar{\mathcal{R}}_v(L)}{v_L}. \quad (115)$$

Again we can summarize these results (substituting back in N_T) as

$$\mathcal{E} = \frac{N\Delta_\Phi^3}{N_T}\sum_n \bar{\alpha}_n^{\mathcal{Q}}\bar{\beta}_n^{\mathcal{Q}} \quad (116)$$

with

$$\bar{\beta}_n^{\mathcal{Q}} = 12\int d^2\hat{n}_1 d^2\hat{n}_2 \bar{\mathcal{M}}_n^{\mathcal{Q}}(\hat{n}_1,\hat{n}_2), \quad (117)$$

and the form of $\bar{\mathcal{M}}_n^{\mathcal{Q}}(\hat{n}_1,\hat{n}_2)$ can be deduced from the equations for $\mathcal{E}^{\rm tot}$ and $\mathcal{E}^{\rm uc}$.

Since there are no line of sight integrals ($\sim \int dr$) for this estimator, the number of operations required in this case is $\mathcal{O}(l^5_{\rm max})$ suggesting that the late-time estimator is much more computationally efficient than the primordial version.

Similarly to the primordial case, there is a reduction in complexity to $\mathcal{O}(l^3_{\rm max})$ in the case that the late-time extra-reduced trispectrum is independent of the diagonal L. This is explained further in Appendix D.

C. T_{NL} estimator

As with the shortcomings of normalizing the quantity f_{NL} of the bispectrum that was addressed in [1], the current method [14] of normalizing the level of non-Gaussianity due to the trispectrum, t_{NL}, poses problems. In particular, the level of non-Gaussianity is found by normalizing the shape function against a central point. More specifically, we can identify this method as setting $S_{\mathcal{T}}(k,k,k,k,k) = 1$ and identifying the normalization N of Eq. (37) as $(50/27)t_{NL}$. In the case of the local model this gives

$$t^{\rm locA}_{NL} = 2.16 f^2_{NL} = 1.5\tau_{NL}, \qquad t^{\rm locB}_{NL} = 1.08 g_{NL}, \quad (118)$$

where we note again that the relationship between τ_{NL} and f_{NL} is only strictly true for single-field inflation. This approach assumes scale invariance and therefore will produce inconsistent results between models peaking or dipping at this central point. Also, this definition is not well defined for models which are not scale invariant, such as feature models, and it is simply not applicable to non-Gaussian signals created at late times, such as those induced by cosmic strings or secondary anisotropies. An alternative measure of the non-Gaussianity is given by comparison of the primordial trispectrum to the local primordial trispectrum, but this approach is not well defined and is essentially an order of magnitude estimation [13].

Therefore, we propose a universally defined trispectrum non-Gaussianity parameter T_{NL} which (i) is a measure of the total observational signal expected for the trispectrum of the model in question and (ii) is normalized for direct comparison with the canonical local model (with $g_{NL} = 0$). We define $\tilde{T}_{NL}$ from an adapted version of the estimator (28) with

$$\tilde{T}_{NL} = \frac{1}{N_T \bar{\mathcal{N}}_{T\rm locA}} \times \sum_{l_im_i} \frac{\langle a_{l_1m_1}a_{l_2m_2}a_{l_3m_3}a_{l_4m_4}\rangle_c (a^{\rm obs}_{l_1m_1}a^{\rm obs}_{l_2m_2}a^{\rm obs}_{l_3m_3}a^{\rm obs}_{l_4m_4})_c}{C_{l_1}C_{l_2}C_{l_3}C_{l_4}}, \quad (119)$$

where N is the appropriate normalization factor for the given model,

$$N_T^2 = \sum_{l_i,L} \frac{(T^{l_1l_2}_{l_3l_4}(L))^2}{(2L+1)C_{l_1}C_{l_2}C_{l_3}C_{l_4}}, \quad (120)$$

and $\bar{\mathcal{N}}_{T\rm locA}$ is the normalization for the local model with $\tau_{NL} = 1$, $g_{NL} = 0$.

$$\bar{\mathcal{N}}^{\,2}_{T\rm locA} = \sum_{l_i,L} \frac{(T^{l_1l_2}_{l_3l_4}(L)^{{\rm loc}(\tau_{NL}=1,g_{NL}=0)})^2}{(2L+1)C_{l_1}C_{l_2}C_{l_3}C_{l_4}}. \quad (121)$$

The $\tilde{T}_{NL}$ estimator will recover τ_{NL} for the local model with $g_{NL} = 0$, while it gives $(\bar{\mathcal{N}}_{T\rm locB}/\bar{\mathcal{N}}_{T\rm locA})g_{NL}$ for the local model with $\tau_{NL} = 0$, where $\bar{\mathcal{N}}_{T\rm locB}$ is the normalization for the local model with $\tau_{NL} = 0$, $g_{NL} = 1$. This coefficient is dependent on $l_{\rm max}$ but is a number of order unity.

Results for primordial models should not depend strongly on the multipole cutoff $l_{\rm max}$. However, diffusion due to Silk damping in the transfer functions ensures that the primordial signal is exponentially suppressed for $l \gtrsim 2000$. Therefore, an appropriate choice for a canonical cutoff is $l_{\rm max} = 2000$. Late-time anisotropies, such as cosmic strings, do not generically fall off exponentially for $l \gtrsim 2000$ but, nonetheless, in the domain $l \lesssim 2000$ we can make a meaningful comparison to the local $\tau_{NL} = 1$, $g_{NL} = 0$ model. Alternative measures must be proposed beyond this domain. As indicated in Appendix A the

normalization factor N_T^2 is a computationally intensive calculation. Instead, we use the approximation $N_T \approx \bar{\mathcal{N}}_{T\mathrm{locA}}(N_{\mathcal{T}}/\bar{\mathcal{N}}_{\mathcal{T}\mathrm{locA}})$, where the subscript $\mathcal{T}$ instead of T refers to using the reduced trispectrum instead of the full trispectrum in the above calculations. With these approximations we need only accurately calculate the full normalization factor in the case of the model with $\tau_{NL} = 1$, $g_{NL} = 0$. Regardless of the accuracy, given the vastly increased speed of the calculation, we adopt this latter convention and define T_{NL}, i.e.

$$T_{NL} = \frac{\bar{\mathcal{N}}_{\mathcal{T}\mathrm{locA}}}{N_{\mathcal{T}}\bar{\mathcal{N}}^2_{T\mathrm{locA}}} \times \sum_{l_i m_i} \frac{\langle a_{l_1 m_1} a_{l_2 m_2} a_{l_3 m_3} a_{l_4 m_4}\rangle_c (a^{\mathrm{obs}}_{l_1 m_1} a^{\mathrm{obs}}_{l_2 m_2} a^{\mathrm{obs}}_{l_3 m_3} a^{\mathrm{obs}}_{l_4 m_4})_c}{C_{l_1} C_{l_2} C_{l_3} C_{l_4}}. \tag{122}$$

The relation between T_{NL} and $\tilde{T}_{NL}$ as well as the accuracy of the above approximation for N_T—which is only a conjecture at present—will be explored further in an upcoming paper. However, we note here that the T_{NL} estimator also recovers τ_{NL} in the case of the local model with $g_{NL} = 0$.

If the CMB trispectrum is not known precisely for the primordial model under study, then we can make an estimate for the normalization factor $N_{\mathcal{T}}$ in (122) using the shape function for the reduced trispectrum $S_{\mathcal{T}}(k_1, k_2, k_3, k_4, K)$. One can obtain a fairly accurate approximation to the relative normalizations in (122) from

$$\hat{N}^2 = F(S_{\mathcal{T}}, S_{\mathcal{T}}) = \int d\mathcal{V}_k S^2_{\mathcal{T}}(k_1, k_2, k_3, k_4, K)\omega(k_1, k_2, k_3, k_4, K), \tag{123}$$

where the appropriate weight function was found in (47) and the domain $\mathcal{V}_k$ is given by (75) and (76). Using $N_{\mathcal{T}}/\bar{\mathcal{N}}_{\mathcal{T}\mathrm{locA}} \approx \hat{N}/\hat{N}_{\mathrm{locA}}$ to approximate $N_{\mathcal{T}}$, we can make a fairly accurate estimate of the level of non-Gaussianity or can renormalize τ_{NL} constraints for different models into compatible constraints in a similar manner to the analysis of f_{NL} constraints in the case of the bispectrum in [1].

VII. RECOVERING THE TRISPECTRUM

A. Recovering the primordial trispectrum

The form of the estimator in (106) suggests that further information may be extracted from the observed trispectrum beyond the τ_{NL} for one specific theoretical model. This is because, through the coefficients $\beta^{\mathcal{Q}}_m$, we have obtained some sort of mode decomposition of the trispectrum of the observational map. Consider the expectation value of $\beta^{\mathcal{Q}}_m$ obtained from an ensemble of maps generated for a particular theoretical model with shape function $S_{\mathcal{T}} = \sum_m \alpha^{\mathcal{Q}}_m \mathcal{Q}_m$. Since the shape function is in terms of the zeroth mode of the Legendre expansion of the primordial trispectrum, we can only hope to recover information about this mode via recovery of the shape function.[4] Using the expression

$$\langle\beta^{\mathcal{Q}}_m\rangle = 12\sum_{l_i m_i}\sum_{LM}\Bigg[\left(\int d\hat{n}_1 Y_{l_1 m_1}(\hat{n}_1) Y_{l_2 m_2}(\hat{n}_1) Y^*_{LM}(\hat{n}_1)\right) \times \left(\int d\hat{n}_2 Y_{l_3 m_3}(\hat{n}_2) Y_{l_4 m_4}(\hat{n}_2) Y_{LM}(\hat{n}_2)\right) \times \int r_1^2 dr_1 r_2^2 dr_2 \mathcal{Q}^{l_1 l_2 l_3 l_4 L}_m(r_1, r_2)\Bigg] \times \frac{\langle a_{l_1 m_1} a_{l_2 m_2} a_{l_3 m_3} a_{l_4 m_4}\rangle_c}{C_{l_1} C_{l_2} C_{l_3} C_{l_4}}, \tag{124}$$

as well as the identity for the Wigner $6j$ symbol in Appendix A, we find, after some algebra,

$$\begin{aligned}\langle\beta^{\mathcal{Q}}_m\rangle = 12\sum_{l_i, L}\int dr_1 dr_2 r_1^2 r_2^2 \mathcal{Q}^{l_1 l_2 l_3 l_4 L}_m(r_1, r_2)\sum_{m'}\alpha^{\mathcal{Q}}_{m'}\Bigg[h^2_{l_1 l_2 L} h^2_{l_3 l_4 L}\int dr_1 dr_2 r_1^2 r_2^2 \mathcal{P}^{l_1 l_2 l_3 l_4 L}_{m'}(r_1, r_2) \\ + \sum_{L'} h_{l_1 l_2 L} h_{l_3 l_4 L} h_{l_1 l_3 L'} h_{l_2 l_4 L'} (-1)^{l_2 + l_3}\begin{Bmatrix} l_1 & l_2 & L \\ l_4 & l_3 & L'\end{Bmatrix}\int dr_1 dr_2 r_1^2 r_2^2 \mathcal{P}^{l_1 l_3 l_2 l_4 L'}_{m'}(r_1, r_2) \\ + \sum_{L'} h_{l_1 l_2 L} h_{l_3 l_4 L} h_{l_1 l_4 L'} h_{l_2 l_3 L'} (-1)^{L + L'}\begin{Bmatrix} l_1 & l_2 & L \\ l_3 & l_4 & L'\end{Bmatrix}\int dr_1 dr_2 r_1^2 r_2^2 \mathcal{P}^{l_1 l_4 l_2 l_3 L'}_{m'}(r_1, r_2)\Bigg] \\ = \sum_{m'}\Gamma_{mm'}\alpha^{\mathcal{Q}}_{m'},\end{aligned} \tag{125}$$

where $\mathcal{P}^{l_1 l_2 l_3 l_4 L}_{m'} = \mathcal{Q}^{l_1 l_2 l_3 l_4 L}_{m'} + \mathcal{Q}^{l_2 l_1 l_3 l_4 L}_{m'} + \mathcal{Q}^{l_1 l_2 l_4 l_3 L}_{m'} + \mathcal{Q}^{l_2 l_1 l_4 l_3 L}_{m'}$. The quantity $\Gamma_{mm'}$ represents a matrix with positions labeled by m, m' and can be inferred readily by the above equation. Inverting the relationship we can recover the $\alpha^{\mathcal{Q}}_m$ via

[4]This is to be somewhat expected since the primordial trispectrum is a six-dimensional quantity whereas the CMB trispectrum is explicitly five dimensional.

$$\alpha_m^{\mathcal{Q}} = \sum_{m'} (\Gamma^{-1})_{mm'} \langle \beta_{m'}^{\mathcal{Q}} \rangle. \tag{126}$$

Therefore, if the decomposition coefficients are found with adequate significance, we can reconstruct the shape function through the expansion

$$S_{\mathcal{T}} = \sum_m \sum_{m'} (\Gamma^{-1})_{mm'} \beta_{m'}^{\mathcal{Q}} \mathcal{Q}_m. \tag{127}$$

This reconstruction will be sufficient to uniquely define the planar case ($\theta_4 = 0$) (as well as the general CMB case in the next section). However, as already discussed, the shape function only gives information about the zeroth Legendre mode of the primordial trispectrum. Therefore, recovery of the full primordial trispectrum is compromised by this degeneracy. However, as we have discussed in Sec. II, this degeneracy may be broken by using other probes of non-Gaussianity, such as galaxy surveys and 21 cm observations. We note also that the calculation of the matrix Γ is computationally intensive due to the presence of the Wigner $6j$ symbols. Nonetheless we include the discussion here for completeness.

B. Recovering the CMB trispectrum

The recovery of the CMB bispectrum from a given observational map is more straightforward (as for the bispectrum). In a similar fashion to the calculation in the case of the primordial trispectrum, we find that

$$\begin{aligned}
\langle \bar{\beta}_n^{\mathcal{Q}} \rangle &= 12 \sum_{l_i m_i} \sum_{LM} \left[\left(\int d\hat{n}_1 Y_{l_1 m_1}(\hat{n}_1) Y_{l_2 m_2}(\hat{n}_1) Y^*_{LM}(\hat{n}_1) \right) \left(\int d\hat{n}_2 Y_{l_3 m_3}(\hat{n}_2) Y_{l_4 m_4}(\hat{n}_2) Y_{LM}(\hat{n}_2) \right) \int r_1^2 dr_1 r_2^2 dr_2 \bar{\mathcal{Q}}_n^{l_1 l_2 l_3 l_4 L}(r_1, r_2) \right] \\
&\quad \times \frac{\langle a_{l_1 m_1} a_{l_2 m_2} a_{l_3 m_3} a_{l_4 m_4} \rangle_c}{\upsilon_{l_1} \upsilon_{l_2} \upsilon_{l_3} \upsilon_{l_4} \upsilon_L \sqrt{C_{l_1} C_{l_2} C_{l_3} C_{l_4}}} \\
\Rightarrow \langle \bar{\beta}_n^{\mathcal{Q}} \rangle &= 12 \sum_{l_i, L} \bar{\mathcal{Q}}_n^{l_1 l_2 l_3 l_4 L} \sum_p \bar{\alpha}_p^{\mathcal{Q}} \left[h^2_{l_1 l_2 L} h^2_{l_3 l_4 L} \mathcal{P}_p^{l_1 l_2 l_3 l_4 L} + \sum_{L'} h_{l_1 l_2 L} h_{l_3 l_4 L} h_{l_1 l_3 L'} h_{l_2 l_4 L'} (-1)^{l_2 + l_3} \begin{Bmatrix} l_1 & l_2 & L \\ l_4 & l_3 & L' \end{Bmatrix} \right. \\
&\quad \left. \times \mathcal{P}_p^{l_1 l_3 l_2 l_4 L'} + \sum_{L'} h_{l_1 l_2 L} h_{l_3 l_4 L} h_{l_1 l_4 L'} h_{l_2 l_3 L'} (-1)^{L + L'} \begin{Bmatrix} l_1 & l_2 & L \\ l_3 & l_4 & L' \end{Bmatrix} \mathcal{P}_p^{l_1 l_4 l_2 l_3 L'} \right] \\
&= \sum_p \bar{\Gamma}_{np} \alpha_p^{\mathcal{Q}},
\end{aligned} \tag{128}$$

where $\bar{\mathcal{Q}}^{l_1 l_2 l_3 l_4 L} = \bar{\mathcal{Q}}_p(l_1) \bar{\mathcal{Q}}_r(l_2) \bar{\mathcal{Q}}_s(l_3) \bar{\mathcal{Q}}_u(l_4) \bar{\mathcal{R}}_v(L)$ and $\mathcal{P}_p^{l_1 l_2 l_3 l_4 L} = \mathcal{Q}_p^{l_1 l_2 l_3 l_4 L} + \mathcal{Q}_p^{l_2 l_1 l_3 l_4 L} + \mathcal{Q}_p^{l_1 l_2 l_4 l_3 L} + \mathcal{Q}_p^{l_2 l_1 l_4 l_3 L}$. Inverting the matrix $\bar{\Gamma}_{np}$ we find

$$\alpha_n^{\mathcal{Q}} = \sum_p \bar{\Gamma}^{-1}_{np} \langle \bar{\beta}_p^{\mathcal{Q}} \rangle. \tag{129}$$

Therefore, if we can measure the coefficients $\bar{\beta}_p^{\mathcal{Q}}$ with significance from a particular experiment, we can reconstruct the trispectrum map using (112),

$$t^{l_1 l_2}_{l_3 l_4}(L) = \frac{\sqrt{C_{l_1} C_{l_2} C_{l_3} C_{l_4}}}{\upsilon_{l_1} \upsilon_{l_2} \upsilon_{l_3} \upsilon_{l_4} \upsilon_L} \sum_{np} \bar{\Gamma}^{-1}_{np} \bar{\beta}_p^{\mathcal{Q}} \bar{\mathcal{Q}}_n. \tag{130}$$

The calculation of the matrix $\bar{\Gamma}$ remains computationally intensive, but it is tractable. We can, in principle, extract the full CMB trispectrum which, together with the extracted CMB bispectrum [1], will prove to be a key test of the Gaussianity of the Universe.

VIII. MAP MAKING

In this section we derive an algorithm for creating a non-Gaussian map with a given trispectrum, developing methods presented for the bispectrum in Ref. [42] and generalized in Ref. [1]. This algorithm is valid in the limit of weak non-Gaussianity.

We define the function

$$T_2[a^G] = \frac{1}{24} \sum_{l_i m_i} T_{l_1 m_1 l_2 m_2 l_3 m_3 l_4 m_4} a^G_{l_1 m_1} a^G_{l_2 m_2} a^G_{l_3 m_3} a^G_{l_4 m_4}, \tag{131}$$

where a^G_{lm} is the Gaussian part of the CMB multipoles, generated using the angular power spectrum C_l, while $T_{l_1 m_1 l_2 m_2 l_3 m_3 l_4 m_4}$ is the given trispectrum of the theoretical model for which simulations are required.

Setting

$$\begin{aligned}
a'_{lm} &= a^G_{lm} + \frac{1}{6} \sum_{l_i m_i} b_{l l_2 l_3} \mathcal{G}^{l l_2 l_3}_{m m_2 m_3} \frac{a^{*G}_{l_2 m_2}}{C_{l_2}} \frac{a^{*G}_{l_3 m_3}}{C_{l_3}} \\
&\quad + \frac{1}{4} \frac{\partial}{\partial a^*_{lm}} T_2[C^{-1} a^G] \\
&= a^G_{lm} + \frac{1}{6} \sum_{l_i m_i} b_{l l_2 l_3} \mathcal{G}^{l l_2 l_3}_{m m_2 m_3} \frac{a^{*G}_{l_2 m_2}}{C_{l_2}} \frac{a^{*G}_{l_3 m_3}}{C_{l_3}} \\
&\quad + \frac{1}{24} \sum_{l_i m_i} T_{l m l_2 m_2 l_3 m_3 l_4 m_4} \frac{a^{*G}_{l_2 m_2}}{C_{l_2}} \frac{a^{*G}_{l_3 m_3}}{C_{l_3}} \frac{a^{*G}_{l_4 m_4}}{C_{l_4}},
\end{aligned} \tag{132}$$

we recover the bispectrum from $\langle a'_{l_1m_1} a'_{l_2m_2} a'_{l_3m_3}\rangle$ (as described in [42]). Next, we calculate the four-point correlator of the a'_{lm}'s and find

$$\langle a'_{l_1m_1} a'_{l_2m_2} a'_{l_3m_3} a'_{l_4m_4}\rangle = \langle a^G_{l_1m_1} a^G_{l_2m_2} a^G_{l_3m_3} a^G_{l_4m_4}\rangle + \left\langle \frac{1}{24}\sum_{l_jm_j} T_{l_1m_1l_bm_bl_cm_cl_dm_d} \frac{a^{*G}_{l_bm_b}}{C_{l_b}} \frac{a^{*G}_{l_cm_c}}{C_{l_c}} \frac{a^{*G}_{l_dm_d}}{C_{l_d}} a^G_{l_2m_2} a^G_{l_3m_3} a^G_{l_4m_4}\right\rangle + \text{permutations}, \tag{133}$$

where $j \in (b, c, d)$. The first term clearly gives the unconnected component of the four-point correlator. We note that the contribution from the bispectrum is zero since the correlator over an odd number of a^G_{lm} vanishes. Evaluating the correlators in the second term on the right-hand side and adding up the different permutations, we find

$$\langle a'_{l_1m_1} a'_{l_2m_2} a'_{l_3m_3} a'_{l_4m_4}\rangle = \langle a^G_{l_1m_1} a^G_{l_2m_2} a^G_{l_3m_3} a^G_{l_4m_4}\rangle + T_{l_1m_1l_2m_2l_3m_3l_4m_4}. \tag{134}$$

This verifies the validity of the use of a'_{lm} to make maps, including the Gaussian, bispectrum, and trispectrum contributions to the model under study.

We observe, using (11), that we may write $T_2[a^G]$ in the form

$$T_2[a^G] = \frac{1}{2}\sum_{l_im_i} \mathcal{T}_{l_1m_1l_2m_2l_3m_3l_4m_4} a^G_{l_1m_1} a^G_{l_2m_2} a^G_{l_3m_3} a^G_{l_4m_4}. \tag{135}$$

Using this formula we may also rewrite the trispectrum contribution to a'_{lm}, which we denote $a^{NG,T}_{lm}$, as

$$a^{NG,T}_{lm} = \frac{1}{24}\sum_{l_im_i} T_{lml_2m_2l_3m_3l_4m_4} \frac{a^{*G}_{l_2m_2}}{C_{l_2}} \frac{a^{*G}_{l_3m_3}}{C_{l_3}} \frac{a^{*G}_{l_4m_4}}{C_{l_4}} = \frac{1}{8}\sum_{l_im_i} (\mathcal{T}_{lml_2m_2l_3m_3l_4m_4} + \mathcal{T}_{l_2m_2lml_3m_3l_4m_4} + \mathcal{T}_{l_2m_2l_3m_3lml_4m_4} + \mathcal{T}_{l_2m_2l_3m_3l_4m_4lm}) \frac{a^{*G}_{l_2m_2}}{C_{l_2}} \frac{a^{*G}_{l_3m_3}}{C_{l_3}} \frac{a^{*G}_{l_4m_4}}{C_{l_4}}. \tag{136}$$

Using the formulas for the extra-reduced trispectrum (23) and the Gaunt integral (14), we note that

$$\mathcal{T}_{l_1m_1l_2m_2l_3m_3l_4m_4} = \sum_{LM}\left(\int d\Omega_{\hat{n}_1} Y_{l_1m_1}(\hat{\mathbf{n}}_1) Y_{l_2m_2}(\hat{\mathbf{n}}_1) Y^*_{LM}(\hat{\mathbf{n}}_1)\right)\left(\int d\Omega_{\hat{n}_2} Y_{l_3m_3}(\hat{\mathbf{n}}_2) Y_{l_4m_4}(\hat{\mathbf{n}}_2) Y_{LM}(\hat{\mathbf{n}}_2)\right) t^{l_1l_2}_{l_3l_4}(L). \tag{137}$$

As an aside, we note that if $t^{l_1l_2}_{l_3l_4}(L)$ is independent of the diagonal L, then we can use Eq. (C11) to write

$$\mathcal{T}_{l_1m_1l_2m_2l_3m_3l_4m_4} = \int d\Omega_{\hat{n}} Y_{l_1m_1}(\hat{\mathbf{n}}) Y_{l_2m_2}(\hat{\mathbf{n}}) Y_{l_3m_3}(\hat{\mathbf{n}}) Y_{l_4m_4}(\hat{\mathbf{n}}) t^{l_1l_2}_{l_3l_4}, \tag{138}$$

where we drop the label L from the extra-reduced trispectrum. This special class of trispectra is explored further in Appendix D.

Denoting the bispectrum contribution to a'_{lm} as $a^{NG,B}_{lm}$ we have verified the following prescription for forming maps, including the bispectrum and trispectrum contributions,

$$a'_{lm} = a^G_{lm} + f_{NL}\tilde{a}^{NG,B}_{lm} + \tau_{NL}\tilde{a}^{NG,T}_{lm}, \tag{139}$$

where we have written $a^{NG,B}_{lm} = f_{NL}\tilde{a}^{NG,B}_{lm}$ and $a^{NG,T}_{lm} = \tau_{NL}\tilde{a}^{NG,T}_{lm}$ to make the size of the respective non-Gaussian components more explicit.

Since the computation of the reduced trispectrum is more efficient using the late-time expression (due to the absence of the line of sight integrals), we write out the formula for $a^{NG,T}_{lm}$ using the late-time mode decomposition. It is straightforward to find the equivalent formula using the primordial expression. Later in the section we present a particular application using the primordial local model of this formalism.

The late-time mode decomposition of the extra-reduced trispectrum $t^{l_1l_2}_{l_3l_4}(L)$—as detailed at the end of Sec. V—may be written as

$$t^{l_1l_2}_{l_3l_4}(L) = \sum_n \tilde{\alpha}^Q_n \bar{\mathcal{Q}}_p(l_1) \bar{\mathcal{Q}}_r(l_2) \bar{\mathcal{Q}}_s(l_3) \bar{\mathcal{Q}}_u(l_4) \bar{\mathcal{R}}_v(L). \tag{140}$$

Using these expressions we have

$$\sum_{l_i m_i} \mathcal{T}_{l m l_2 m_2 l_3 m_3 l_4 m_4} \frac{a^{*G}_{l_2 m_2}}{C_{l_2}} \frac{a^{*G}_{l_3 m_3}}{C_{l_3}} \frac{a^{*G}_{l_4 m_4}}{C_{l_4}}$$
$$= \sum_n \bar{\alpha}^{\mathcal{Q}}_n \int d\Omega_{\hat{\mathbf{n}}_1} d\Omega_{\hat{\mathbf{n}}_2} Y_{lm}(\hat{\mathbf{n}}_1) \bar{\mathcal{Q}}_p(l) \bar{\mathcal{M}}_r(\hat{\mathbf{n}}_1) \bar{\mathcal{M}}_s(\hat{\mathbf{n}}_2) \times \bar{\mathcal{M}}_u(\hat{\mathbf{n}}_2) \bar{\mathcal{N}}_v(\hat{\mathbf{n}}_1, \hat{\mathbf{n}}_2), \quad (141)$$

where

$$\bar{\mathcal{M}}_r(\hat{\mathbf{n}}_1) = \sum_{l_2 m_2} \frac{Y_{l_2 m_2}(\hat{\mathbf{n}}_1) a^{*G}_{l_2 m_2}}{C_{l_2}} \bar{\mathcal{Q}}_r(l_2),$$
$$\bar{\mathcal{N}}_v(\hat{\mathbf{n}}_1, \hat{\mathbf{n}}_2) = \bar{\mathcal{N}}_v(\hat{\mathbf{n}}_2, \hat{\mathbf{n}}_1) = \sum_{LM} Y^*_{LM}(\hat{\mathbf{n}}_1) Y_{LM}(\hat{\mathbf{n}}_2) \bar{\mathcal{R}}_v(L). \quad (142)$$

Evaluating, in a similar way, the other terms in Eq. (136) we find

$$a^{NG,T}_{lm} = \frac{1}{8} \sum_n \bar{\alpha}^{\mathcal{Q}}_n \int d\Omega_{\hat{\mathbf{n}}_1} d\Omega_{\hat{\mathbf{n}}_2} Y_{lm}(\hat{\mathbf{n}}_1) [(\bar{\mathcal{Q}}_p(l) \bar{\mathcal{M}}_r(\hat{\mathbf{n}}_1) + \bar{\mathcal{Q}}_r(l) \bar{\mathcal{M}}_p(\hat{\mathbf{n}}_1)) \bar{\mathcal{M}}_s(\hat{\mathbf{n}}_2) \bar{\mathcal{M}}_u(\hat{\mathbf{n}}_2) + (\bar{\mathcal{Q}}_s(l) \bar{\mathcal{M}}_u(\hat{\mathbf{n}}_1) + \bar{\mathcal{Q}}_u(l) \bar{\mathcal{M}}_s(\hat{\mathbf{n}}_1)) \bar{\mathcal{M}}_p(\hat{\mathbf{n}}_2) \bar{\mathcal{M}}_r(\hat{\mathbf{n}}_2)] \bar{\mathcal{N}}_v(\hat{\mathbf{n}}_1, \hat{\mathbf{n}}_2). \quad (143)$$

As emphasized in [1] the condition that the map has the power spectrum C_l specified in the input will only be satisfied if the power spectrum of the non-Gaussian components C^{NG}_l is small. Therefore, one has to ascertain that spuriously large C^{NG}_l contributions do not affect the overall power spectrum significantly. We will discuss the implementation of the algorithm presented here in an upcoming paper [40].

Application to the local model

The reduced trispectrum for the local model, as shown in Sec. IV, is made up of two terms which we denote locA and locB. As shown in [43]—and can be deduced from Sec. IV—the extra-reduced trispectra may be written as

$$t^{l_1 l_2}_{l_3 l_4}(L)^{\mathrm{locA}} = \frac{25}{9} \tau_{NL} \int dr_1 dr_2 r_1^2 r_2^2 F_L(r_1, r_2) \alpha_{l_1}(r_1) \times \beta_{l_2}(r_1) \alpha_{l_3}(r_2) \beta_{l_4}(r_2), \quad (144)$$

$$t^{l_1 l_2}_{l_3 l_4}(L)^{\mathrm{locB}} = g_{NL} \int dr r^2 \beta_{l_2}(r) \beta_{l_4}(r) (\mu_{l_1}(r) \beta_{l_3}(r) + \beta_{l_1}(r) \mu_{l_3}(r)), \quad (145)$$

where

$$F_L(r_1, r_2) = \frac{2}{\pi} \int K^2 dK P_\Phi(K) j_L(K r_1) j_L(K r_2),$$
$$\alpha_l(r) = \mu_l(r) = \frac{2}{\pi} \int k^2 dk \Delta_l(k) j_l(k r), \quad (146)$$
$$\beta_l(r) = \frac{2}{\pi} \int k^2 dk P_\Phi(k) \Delta_l(k) j_l(k r).$$

Using these formulas, and exploiting that the locB trispectrum is independent of the diagonal L with Eq. (138), we find

$$\sum_{l_i m_i} \mathcal{T}^{\mathrm{locA}}_{l m l_2 m_2 l_3 m_3 l_4 m_4} \frac{a^{*G}_{l_2 m_2}}{C_{l_2}} \frac{a^{*G}_{l_3 m_3}}{C_{l_3}} \frac{a^{*G}_{l_4 m_4}}{C_{l_4}}$$
$$= \frac{25}{9} \tau_{NL} \int dr_1 dr_2 r_1^2 r_2^2 \alpha_l(r_1) \int d\Omega_{\hat{\mathbf{n}}_1} d\Omega_{\hat{\mathbf{n}}_2} Y_{lm}(\hat{\mathbf{n}}_1) \times \mathcal{M}_F(\hat{\mathbf{n}}_1, \hat{\mathbf{n}}_2, r_1, r_2) \mathcal{M}_\beta(\hat{\mathbf{n}}_1, r_1) \mathcal{M}_\alpha(\hat{\mathbf{n}}_2, r_2) \times \mathcal{M}_\beta(\hat{\mathbf{n}}_2, r_2), \quad (147)$$

$$\sum_{l_i m_i} \mathcal{T}^{\mathrm{locB}}_{l m l_2 m_2 l_3 m_3 l_4 m_4} \frac{a^{*G}_{l_2 m_2}}{C_{l_2}} \frac{a^{*G}_{l_3 m_3}}{C_{l_3}} \frac{a^{*G}_{l_4 m_4}}{C_{l_4}}$$
$$= g_{NL} \int dr r^2 \int d\Omega_{\hat{\mathbf{n}}} Y_{lm}(\hat{\mathbf{n}}) [\mu_l(r) \mathcal{M}_\beta(\hat{\mathbf{n}}, r) + \beta_l(r) \mathcal{M}_\mu(\hat{\mathbf{n}}, r)] \mathcal{M}_\beta(\hat{\mathbf{n}}, r) \mathcal{M}_\beta(\hat{\mathbf{n}}, r), \quad (148)$$

where

$$\mathcal{M}_\alpha(\hat{\mathbf{n}}, r) = \mathcal{M}_\mu(\hat{\mathbf{n}}, r) = \sum_{lm} \alpha_l(r) \frac{Y_{lm}(\hat{\mathbf{n}}) a^{*G}_{lm}}{C_l},$$
$$\mathcal{M}_\beta(\hat{\mathbf{n}}, r) = \sum_{lm} \beta_l(r) \frac{Y_{lm}(\hat{\mathbf{n}}) a^{*G}_{lm}}{C_l}, \quad (149)$$
$$\mathcal{M}_F(\hat{\mathbf{n}}_1, \hat{\mathbf{n}}_2, r_1, r_2) = \sum_{LM} Y^*_{LM}(\hat{\mathbf{n}}_1) Y_{LM}(\hat{\mathbf{n}}_2) F_L(r_1, r_2).$$

We similarly find the other terms in (136) to get

$$(a^{NG,T}_{lm})_{\mathrm{locA}} = \frac{25}{36} \tau_{NL} \int dr_1 dr_2 r_1^2 r_2^2 \Big[\alpha_l(r_1) \int d\Omega_{\hat{\mathbf{n}}_1} d\Omega_{\hat{\mathbf{n}}_2} Y_{lm}(\hat{\mathbf{n}}_1) \mathcal{M}_\beta(\hat{\mathbf{n}}_1, r_1) + \beta_l(r_1) \int d\Omega_{\hat{\mathbf{n}}_1} d\Omega_{\hat{\mathbf{n}}_2} Y_{lm}(\hat{\mathbf{n}}_1) \mathcal{M}_\alpha(\hat{\mathbf{n}}_1, r_1) \Big] \times \mathcal{M}_\alpha(\hat{\mathbf{n}}_2, r_2) \mathcal{M}_\beta(\hat{\mathbf{n}}_2, r_2) \mathcal{M}_F(\hat{\mathbf{n}}_1, \hat{\mathbf{n}}_2, r_1, r_2), \quad (150)$$

$$(a_{lm}^{NG,T})_{\rm locB} = \frac{1}{4} g_{NL} \int dr r^2 \Big[\mu_l(r) \int d\Omega_{\hat{\mathbf{n}}} Y_{lm}(\hat{\mathbf{n}}) \mathcal{M}_\beta(\hat{\mathbf{n}}, r) \mathcal{M}_\beta(\hat{\mathbf{n}}, r) \mathcal{M}_\beta(\hat{\mathbf{n}}, r) + \beta_l(r) \int d\Omega_{\hat{\mathbf{n}}} Y_{lm}(\hat{\mathbf{n}}) (3 \mathcal{M}_\beta(\hat{\mathbf{n}}, r) \mathcal{M}_\mu(\hat{\mathbf{n}}, r) \mathcal{M}_\beta(\hat{\mathbf{n}}, r)) \Big]. \quad (151)$$

In the case of the bispectrum, direct implementation of the explicitly separable local shape results in spuriously large C_l^{NG} contributions. However, it was found that using the eigenmode expansion in Ref. [1] was much more robust, circumventing such effects, because of the bounded nature of the polynomial eigenmodes. This improvement is expected to occur for the trispectrum. An alternative method is to regularize the expressions given here by eliminating pathological terms, while leaving the final trispectrum of the map unchanged. For arbitrary separable trispectra (unlike the eigenmode expansion), convergence must be achieved by hand on a case-by-case basis.

IX. CONCLUSIONS

We have described in this paper two comprehensive pipelines for the analysis of general primordial or CMB trispectra. The methods are based on mode expansions, exploiting a complete orthonormal eigenmode basis to efficiently decompose arbitrary trispectra into a separable polynomial expansion. These separable mode expansions allow for a reduction of the computational overhead to tractable levels, regardless of whether the reduced trispectrum is being computed at Planck resolution or we are directly finding an estimator for the size of the trispectrum from a real data set. A shape decomposition has been described allowing for a visualization of a scale-invariant reduced trispectrum on particular slices.

We have presented a correlator for comparing trispectra. We have also defined a correlator for comparing the shape functions, which is expected to closely approximate the former. However, the main purpose of this paper was to present a detailed theoretical framework for finding an estimator for the size of the trispectrum using separable eigenmode expansions. Using this efficient method for finding an estimator for the trispectrum, we have defined a universal measure T_{NL} which will allow for consistent comparison between theoretical models. This measure can be calculated for both primordial models and late-time models, e.g. due to active models such as cosmic strings. The completeness of the orthogonal eigenmodes should allow for a reconstruction of the full CMB trispectrum from the data, assuming the presence of a sufficiently significant non-Gaussian signal. We have also detailed an algorithm for producing non-Gaussian simulations with a given power spectrum, bispectrum, and trispectrum. The implementation of these methods will be discussed in a future publication [40]. Clearly, the full implementation of the primordial and late-time pipelines represents a significant challenge. However, the generality and robustness of the methodology described here indicates that there is an intriguing possibility of exploring and constraining a wide class of non-Gaussian models using the trispectrum.

ACKNOWLEDGMENTS

We are very grateful for many informative and illuminating discussions with Xingang Chen and Michele Liguori. We also thank Sébastien Renaux-Petel for comments on an earlier version of this paper. E. P. S. and J. R. F. were supported by STFC Grant No. ST/F002998/1 and the Centre for Theoretical Cosmology. D. M. R. was supported by EPSRC, the Isaac Newton Trust, and the Cambridge European Trust.

APPENDIX A: NORMALIZATION FACTOR

Clearly the appropriate normalization factor for the estimator (28) is of the form

$$N_{T'} = \sum_{l_i m_i} \frac{\langle a_{l_1 m_1} a_{l_2 m_2} a_{l_3 m_3} a_{l_4 m_4} \rangle_c \langle a_{l_1 m_1} a_{l_2 m_2} a_{l_3 m_3} a_{l_4 m_4} \rangle_c}{C_{l_1} C_{l_2} C_{l_3} C_{l_4}}.$$

In order to relate this to N_T expressed in (29) we use Eq. (7) to expand $N_{T'}$ in the form

$$N_{T'} = \sum_{l_i L L'} \sum_{m_i M M'} \frac{1}{C_{l_1} C_{l_2} C_{l_3} C_{l_4}} (-1)^M \begin{pmatrix} l_1 & l_2 & L \\ m_1 & m_2 & -M \end{pmatrix} \times \begin{pmatrix} l_3 & l_4 & L \\ m_3 & m_4 & M \end{pmatrix} T^{l_1 l_2}_{l_3 l_4}(L) (-1)^{M'} \times \begin{pmatrix} l_1 & l_2 & L' \\ m_1 & m_2 & -M' \end{pmatrix} \begin{pmatrix} l_3 & l_4 & L' \\ m_3 & m_4 & M' \end{pmatrix} T^{l_1 l_2}_{l_3 l_4}(L').$$

Now, using

$$\sum_{m_1 m_2} \begin{pmatrix} l_1 & l_2 & L \\ m_1 & m_2 & -M \end{pmatrix} \begin{pmatrix} l_1 & l_2 & L' \\ m_1 & m_2 & -M' \end{pmatrix} = \frac{\delta_{L,L'} \delta_{M,M'}}{2L+1},$$
$$\sum_{M} \sum_{m_3 m_4} \begin{pmatrix} l_3 & l_4 & L \\ m_3 & m_4 & M \end{pmatrix} \begin{pmatrix} l_3 & l_4 & L \\ m_3 & m_4 & M \end{pmatrix} = 1, \quad (A1)$$

we find that

$$N_{T'} = \sum_{l_i, L} \frac{T^{l_1 l_2}_{l_3 l_4}(L) T^{l_1 l_2}_{l_3 l_4}(L)}{(2L+1) C_{l_1} C_{l_2} C_{l_3} C_{l_4}} = N_T.$$

This verifies the use of Eq. (29) to normalize the estimator (28).

We can expand N_T in terms of the reduced trispectrum using

$$N_T = 12\sum_{l_i m_i} \frac{\mathcal{T}_{l_1 m_1 l_2 m_2 l_3 m_3 l_4 m_4} T_{l_1 m_1 l_2 m_2 l_3 m_3 l_4 m_4}}{C_{l_1} C_{l_2} C_{l_3} C_{l_4}}. \quad \text{(A2)}$$

Then with the identity for the Wigner $6j$ symbol (see the Appendix in [34]),

$$\begin{Bmatrix} a & b & e \\ c & d & f \end{Bmatrix} = \sum_{\alpha\beta\gamma}\sum_{\delta\epsilon\phi}(-1)^{e+f+\epsilon+\phi}\begin{pmatrix} a & b & e \\ \alpha & \beta & \epsilon \end{pmatrix} \times\begin{pmatrix} c & d & e \\ \gamma & \delta & -\epsilon \end{pmatrix}\begin{pmatrix} a & d & f \\ \alpha & \delta & -\phi \end{pmatrix} \times\begin{pmatrix} c & b & f \\ \gamma & \beta & \phi \end{pmatrix}, \quad \text{(A3)}$$

the identities (A1), and relations for P in (8) and (9), we find that

$$N_T = 12\sum_{l_i,L}\frac{\mathcal{T}^{l_1 l_2}_{l_3 l_4}(L)}{C_{l_1} C_{l_2} C_{l_3} C_{l_4}}\left(\frac{P^{l_1 l_2}_{l_3 l_4}(L)}{2L+1} + \sum_{L'}(-1)^{l_2+l_3} \times\begin{Bmatrix} l_1 & l_2 & L \\ l_4 & l_3 & L' \end{Bmatrix} P^{l_1 l_3}_{l_2 l_4}(L') + \sum_{L'}(-1)^{L+L'} \times\begin{Bmatrix} l_1 & l_2 & L \\ l_3 & l_4 & L' \end{Bmatrix} P^{l_1 l_4}_{l_3 l_2}(L')\right). \quad \text{(A4)}$$

Because of the presence of the $6j$ symbols the calculation of N_T is computationally very expensive, in general.

APPENDIX B: OPTIMAL ESTIMATOR

When non-Gaussianity is weak we can exploit the multivariate Edgeworth expansion [37] around the Gaussian probability distribution function (PDF), $P^G(a)$, i.e.

$$P(a) = \Bigg[1 - \sum_{l_i m_i}\langle a_{l_1 m_1} a_{l_2 m_2} a_{l_3 m_3}\rangle \frac{\partial}{\partial a_{l_1 m_1}}\frac{\partial}{\partial a_{l_2 m_2}}\frac{\partial}{\partial a_{l_3 m_3}} + \sum_{l_i m_i}\langle a_{l_1 m_1} a_{l_2 m_2} a_{l_3 m_3} a_{l_4 m_4}\rangle_c \frac{\partial}{\partial a_{l_1 m_1}}\frac{\partial}{\partial a_{l_2 m_2}} \times \frac{\partial}{\partial a_{l_3 m_3}}\frac{\partial}{\partial a_{l_4 m_4}} + \ldots\Bigg] P^G(a), \quad \text{(B1)}$$

where the Gaussian PDF is given by

$$P^G(a) = \frac{e^{-(1/2)\sum_{lm}\sum_{l'm'} a_{lm}(C^{-1})_{lm,l'm'}a_{l'm'}}}{(2\pi)^{N/2}|C|^{1/2}} \quad \text{(B2)}$$

with $C_{lm,l'm'} = \langle a_{lm} a_{l'm'}\rangle$ and N the number of l and m. Maximizing over the three-point correlator results in the optimal bispectrum estimator. Here we will ignore this term (setting it to zero for convenience) and concentrate on the four-point correlator. We find

$$P(a) = \Bigg[1 + \sum_{l_i m_i}\langle a_{l_1 m_1} a_{l_2 m_2} a_{l_3 m_3} a_{l_4 m_4}\rangle_c \times ((C^{-1}a)_{l_1 m_1}(C^{-1}a)_{l_2 m_2}(C^{-1}a)_{l_3 m_3}(C^{-1}a)_{l_4 m_4} - 6(C^{-1})_{l_2 m_2, l_1 m_1}(C^{-1}a)_{l_3 m_3}(C^{-1}a)_{l_4 m_4} + 3(C^{-1})_{l_1 m_1, l_2 m_2}(C^{-1})_{l_3 m_3, l_4 m_4})\Bigg] P^G(a), \quad \text{(B3)}$$

where $(C^{-1}a)_{lm} = \sum_{l'm'} C^{-1}_{l'm',lm} a_{l'm'}$. Parametrizing the size of the trispectrum by $\mathcal{E}$, we wish to maximize the PDF with respect to this. We assume that $(a_{l_1 m_1} a_{l_2 m_2} a_{l_3 m_3} a_{l_4 m_4})_c \propto \mathcal{E}$ such that the second term is proportional to $\mathcal{E}$. Maximizing the PDF means that we wish to set $(dP/d\mathcal{E}) = 0$, such that the Taylor expansion about $\mathcal{E} = 0$ reads

$$P(a) = \left[1 + \frac{d(P/P^G)}{d\mathcal{E}}\mathcal{E} + \frac{1}{2}\frac{d^2(P/P^G)}{d\mathcal{E}^2}\mathcal{E}^2 + \ldots\right]P^G(a) \approx \left[1 + \frac{1}{2}\frac{d^2(P/P^G)}{d\mathcal{E}^2}\mathcal{E}^2\right]P^G(a). \quad \text{(B4)}$$

Since

$$\frac{d^2P}{d\mathcal{E}^2} \propto 2\sum_{l_i m_i}\langle a_{l_1 m_1} a_{l_2 m_2} a_{l_3 m_3} a_{l_4 m_4}\rangle_c (C^{-1})_{l_1 m_1, l'_1 m'_1} \times (C^{-1})_{l_2 m_2, l'_2 m'_2}(C^{-1})_{l_3 m_3, l'_3 m'_3}(C^{-1})_{l_4 m_4, l'_4 m'_4} \times (a_{l'_1 m'_1} a_{l'_2 m'_2} a_{l'_3 m'_3} a_{l'_4 m'_4})_c$$

we find that the estimator is maximized by setting (with an appropriate choice of proportionality constant)

$$\mathcal{E} = \frac{f_{\rm sky}}{\tilde{N}}\sum_{l_i m_i}\langle a_{l_1 m_1} a_{l_2 m_2} a_{l_3 m_3} a_{l_4 m_4}\rangle_c ((C^{-1}a)_{l_1 m_1}(C^{-1}a)_{l_2 m_2} \times (C^{-1}a)_{l_3 m_3}(C^{-1}a)_{l_4 m_4} - 6(C^{-1})_{l_1 m_1, l_2 m_2}(C^{-1}a)_{l_3 m_3} \times (C^{-1}a)_{l_4 m_4} + 3(C^{-1})_{l_1 m_1, l_2 m_2}(C^{-1})_{l_3 m_3, l_4 m_4}), \quad \text{(B5)}$$

where

$$\tilde{N} = \sum_{l_i m_i}\langle a_{l_1 m_1} a_{l_2 m_2} a_{l_3 m_3} a_{l_4 m_4}\rangle_c (C^{-1})_{l_1 m_1, l'_1 m'_1}(C^{-1})_{l_2 m_2, l'_2 m'_2} \times (C^{-1})_{l_3 m_3, l'_3 m'_3}(C^{-1})_{l_4 m_4, l'_4 m'_4}(a_{l'_1 m'_1} a_{l'_2 m'_2} a_{l'_3 m'_3} a_{l'_4 m'_4})_c.$$

APPENDIX C: NONOPTIMAL ESTIMATORS—SKEWNESS AND KURTOSIS

The deviation from non-Gaussianity may be measured in a nonoptimal way by estimating the departure of the one-point PDF from Gaussian behavior. This deviation may be measured in terms of the skewness and kurtosis. The skewness is given by

$$g_1 = \frac{\langle (\frac{\Delta T}{T}(\hat{n}))^3 \rangle}{(\langle (\frac{\Delta T}{T}(\hat{n}))^2 \rangle)^{3/2}}, \tag{C1}$$

while the kurtosis is given by (35). Using (1) we evaluate the variance as

$$\left\langle \left(\frac{\Delta T}{T}(\hat{n})\right)^2 \right\rangle = \sum_{l'm'} \sum_{lm} \int \frac{d\Omega_{\hat{n}}}{4\pi} \langle a^*_{l'm'} a_{lm} \rangle Y^*_{l'm'}(\hat{\mathbf{n}}) Y_{lm}(\hat{\mathbf{n}}) = \frac{1}{4\pi} \sum_{lm} \langle a^*_{lm} a_{lm} \rangle = \frac{\sum_l (2l+1) C_l}{4\pi}. \tag{C2}$$

The three-point temperature correlator is similarly given by

$$\left\langle \left(\frac{\Delta T}{T}(\hat{n})\right)^3 \right\rangle = \sum_{l_i m_i} \langle a_{l_1 m_1} a_{l_2 m_2} a_{l_3 m_3} \rangle \times \int \frac{d\Omega_{\hat{n}}}{4\pi} Y_{l_1 m_1}(\hat{\mathbf{n}}) Y_{l_2 m_2}(\hat{\mathbf{n}}) Y_{l_3 m_3}(\hat{\mathbf{n}}) = \frac{1}{4\pi} \sum_{l_i m_i} (\mathcal{G}^{l_1 l_2 l_3}_{m_1 m_2 m_3})^2 b_{l_1 l_2 l_3}, \tag{C3}$$

where $\mathcal{G}^{l_1 l_2 l_3}_{m_1 m_2 m_3}$ is the Gaunt integral and $b_{l_1 l_2 l_3}$ is the reduced bispectrum. The Gaunt integral is given by

$$\mathcal{G}^{l_1 l_2 l_3}_{m_1 m_2 m_3} = h_{l_1 l_2 l_3} \begin{pmatrix} l_1 & l_2 & l_3 \\ m_1 & m_2 & m_3 \end{pmatrix}. \tag{C4}$$

Using Eq. (A1) we can simplify this expression to get

$$\left\langle \left(\frac{\Delta T}{T}(\hat{n})\right)^3 \right\rangle = \frac{1}{4\pi} \sum_{l_i} h^2_{l_1 l_2 l_3} b_{l_1 l_2 l_3}. \tag{C5}$$

Next, in order to evaluate the kurtosis we calculate the quantity

$$\begin{aligned} K &= \left\langle \left(\frac{\Delta T}{T}(\hat{n})\right)^4 \right\rangle - 3\left(\left\langle \left(\frac{\Delta T}{T}(\hat{n})\right)^2 \right\rangle \right)^2 \\ &= \sum_{l_i m_i} \langle a_{l_1 m_1} a_{l_2 m_2} a_{l_3 m_3} a_{l_4 m_4} \rangle \int \frac{d\Omega_{\hat{n}}}{4\pi} Y_{l_1 m_1}(\hat{\mathbf{n}}) Y_{l_2 m_2}(\hat{\mathbf{n}}) Y_{l_3 m_3}(\hat{\mathbf{n}}) Y_{l_4 m_4}(\hat{\mathbf{n}}) \\ &\quad - \sum_{l_i m_i} \int \frac{d\Omega_{\hat{n}_1}}{4\pi} \frac{d\Omega_{\hat{n}_2}}{4\pi} \langle a_{l_1 m_1} a_{l_2 m_2} \rangle \langle a_{l_3 m_3} a_{l_4 m_4} \rangle Y_{l_1 m_1}(\hat{\mathbf{n}}_1) Y_{l_2 m_2}(\hat{\mathbf{n}}_1) Y_{l_3 m_3}(\hat{\mathbf{n}}_2) Y_{l_4 m_4}(\hat{\mathbf{n}}_2) \\ &\quad - \sum_{l_i m_i} \int \frac{d\Omega_{\hat{n}_1}}{4\pi} \frac{d\Omega_{\hat{n}_2}}{4\pi} \langle a_{l_1 m_1} a_{l_3 m_3} \rangle \langle a_{l_2 m_2} a_{l_4 m_4} \rangle Y_{l_1 m_1}(\hat{\mathbf{n}}_1) Y_{l_3 m_3}(\hat{\mathbf{n}}_1) Y_{l_2 m_2}(\hat{\mathbf{n}}_2) Y_{l_4 m_4}(\hat{\mathbf{n}}_2) \\ &\quad - \sum_{l_i m_i} \int \frac{d\Omega_{\hat{n}_1}}{4\pi} \frac{d\Omega_{\hat{n}_2}}{4\pi} \langle a_{l_1 m_1} a_{l_4 m_4} \rangle \langle a_{l_2 m_2} a_{l_3 m_3} \rangle Y_{l_1 m_1}(\hat{\mathbf{n}}_1) Y_{l_4 m_4}(\hat{\mathbf{n}}_1) Y_{l_2 m_2}(\hat{\mathbf{n}}_2) Y_{l_3 m_3}(\hat{\mathbf{n}}_2), \end{aligned} \tag{C6}$$

where the final three terms are clearly equivalent. Using

$$\begin{aligned} \langle a_{l_1 m_1} a_{l_2 m_2} a_{l_3 m_3} a_{l_4 m_4} \rangle &= \langle a_{l_1 m_1} a_{l_2 m_2} a_{l_3 m_3} a_{l_4 m_4} \rangle_c + \langle a_{l_1 m_1} a_{l_2 m_2} \rangle \langle a_{l_3 m_3} a_{l_4 m_4} \rangle + \langle a_{l_1 m_1} a_{l_3 m_3} \rangle \langle a_{l_2 m_2} a_{l_4 m_4} \rangle \\ &\quad + \langle a_{l_1 m_1} a_{l_4 m_4} \rangle \langle a_{l_2 m_2} a_{l_3 m_3} \rangle, \end{aligned} \tag{C7}$$

it can be shown after some algebra that

$$K = \frac{1}{4\pi} \sum_{l_i m_i} \langle a_{l_1 m_1} a_{l_2 m_2} a_{l_3 m_3} a_{l_4 m_4} \rangle_c \times \int d\Omega_{\hat{n}} Y_{l_1 m_1}(\hat{\mathbf{n}}) Y_{l_2 m_2}(\hat{\mathbf{n}}) Y_{l_3 m_3}(\hat{\mathbf{n}}) Y_{l_4 m_4}(\hat{\mathbf{n}}). \tag{C8}$$

From Eq. (11) this may be written in terms of the reduced trispectrum as

$$K = \frac{12}{4\pi} \sum_{l_i m_i} \mathcal{T}_{l_1 m_1 l_2 m_2 l_3 m_3 l_4 m_4} \int d\Omega_{\hat{n}} Y_{l_1 m_1}(\hat{\mathbf{n}}) Y_{l_2 m_2}(\hat{\mathbf{n}}) \times Y_{l_3 m_3}(\hat{\mathbf{n}}) Y_{l_4 m_4}(\hat{\mathbf{n}}). \tag{C9}$$

Next, noting that the product of two spherical harmonics can be written as

$$Y_{l_1 m_1}(\hat{n}) Y_{l_2 m_2}(\hat{n}) = \sum_{L' M'} h_{l_1 l_2 L'} \begin{pmatrix} l_1 & l_2 & L' \\ m_1 & m_2 & -M' \end{pmatrix} \times (-1)^{M'} Y_{L' M'}(\hat{n}) \tag{C10}$$

and Eq. (14), we find

$$\int d\Omega_{\hat{n}} Y_{l_1 m_1}(\hat{\mathbf{n}}) Y_{l_2 m_2}(\hat{\mathbf{n}}) Y_{l_3 m_3}(\hat{\mathbf{n}}) Y_{l_4 m_4}(\hat{\mathbf{n}}) = \sum_{L' M'} (-1)^{M'} h_{l_1 l_2 L'} h_{l_3 l_4 L'} \begin{pmatrix} l_1 & l_2 & L' \\ m_1 & m_2 & -M' \end{pmatrix} \times \begin{pmatrix} l_3 & l_4 & L' \\ m_3 & m_4 & M' \end{pmatrix}. \quad \text{(C11)}$$

Finally, using Eq. (10) for the reduced trispectrum, the orthogonality relation between Wigner $3j$ functions as expressed in (18), and the extra-reduced trispectrum (23), we find

$$K = \frac{12}{4\pi} \sum_{l_i, L} \frac{h_{l_1 l_2 L} h_{l_3 l_4 L}}{2L+1} \mathcal{T}^{l_1 l_2}_{l_3 l_4}(L) = \frac{12}{4\pi} \sum_{l_i, L} \frac{h^2_{l_1 l_2 L} h^2_{l_3 l_4 L}}{2L+1} t^{l_1 l_2}_{l_3 l_4}(L). \quad \text{(C12)}$$

In summary, the skewness and kurtosis are given, respectively, by

$$g_1 = \sqrt{4\pi} \frac{\sum_{l_i} h^2_{l_1 l_2 l_3} b_{l_1 l_2 l_3}}{(\sum_l (2l+1) C_l)^{3/2}}, \quad \text{(C13)}$$

$$g_2 = \frac{48\pi \sum_{l_i, L} h^2_{l_1 l_2 L} h^2_{l_3 l_4 L} t^{l_1 l_2}_{l_3 l_4}(L)/(2L+1)}{(\sum_l (2l+1) C_l)^2}. \quad \text{(C14)}$$

APPENDIX D: SPECIAL CASE OF THE TRISPECTRUM INDEPENDENT OF THE DIAGONAL

Suppose that the primordial reduced trispectrum is independent of the diagonal K. In particular, we write $\mathcal{T}_{\Phi,0}(k_1, k_2, k_3, k_4; K) = \mathcal{T}_{\Phi,0}(k_1, k_2, k_3, k_4)$. In that case the extra-reduced trispectrum [see (23) and (24)] becomes

$$t^{l_1 l_2}_{l_3 l_4}(L) = \left(\frac{2}{\pi}\right)^5 \int (k_1 k_2 k_3 k_4 K)^2 dk_1 dk_2 dk_3 dk_4 dK r_1^2 dr_1 r_2^2 dr_2 j_L(K r_1) j_L(K r_2) [j_{l_1}(k_1 r_1) \Delta_{l_1}(k_1)][j_{l_2}(k_2 r_1) \Delta_{l_2}(k_2)] \times [j_{l_3}(k_3 r_2) \Delta_{l_3}(k_3)][j_{l_4}(k_4 r_2) \Delta_{l_4}(k_4)] \mathcal{T}_{\Phi,0}(k_1, k_2, k_3, k_4). \quad \text{(D1)}$$

Next, using Eq. (61) we find

$$\int dK K^2 j_L(K r_1) j_L(K r_2) = \frac{\pi}{2 r_2^2} \delta(r_2 - r_1). \quad \text{(D2)}$$

This implies that

$$t^{l_1 l_2}_{l_3 l_4}(L) = \left(\frac{2}{\pi}\right)^4 \int (k_1 k_2 k_3 k_4)^2 dk_1 dk_2 dk_3 dk_4 r_1^2 dr_1 [j_{l_1}(k_1 r_1) \Delta_{l_1}(k_1)][j_{l_2}(k_2 r_1) \Delta_{l_2}(k_2)][j_{l_3}(k_3 r_1) \Delta_{l_3}(k_3)] \times [j_{l_4}(k_4 r_1) \Delta_{l_4}(k_4)] \mathcal{T}_{\Phi,0}(k_1, k_2, k_3, k_4); \quad \text{(D3)}$$

i.e. we only have one line of sight integral. This expression also shows that, if the primordial trispectrum is independent of the diagonal K, then $t^{l_1 l_2}_{l_3 l_4}(L)$ is independent of L. We can exploit this property in our estimators. From Eqs. (10), (23), and (14) for the Gaunt integral (which we denote here in the form $\mathcal{G}^{l_1 l_2 l_3}_{m_1 m_2 m_3}$) we have

$$\mathcal{T}_{l_1 m_1 l_2 m_2 l_3 m_3 l_4 m_4} = \sum_{LM} (-1)^M \mathcal{G}^{l_1 l_2 L}_{m_1 m_2 - M} \mathcal{G}^{l_3 l_4 L}_{m_3 m_4 M} t^{l_1 l_2}_{l_3 l_4}(L). \quad \text{(D4)}$$

If the extra-reduced trispectrum is independent of L we can use Eq. (C11) to write

$$\mathcal{T}_{l_1 m_1 l_2 m_2 l_3 m_3 l_4 m_4} = \int d\Omega_{\hat{n}} Y_{l_1 m_1}(\hat{\mathbf{n}}) Y_{l_2 m_2}(\hat{\mathbf{n}}) Y_{l_3 m_3}(\hat{\mathbf{n}}) \times Y_{l_4 m_4}(\hat{\mathbf{n}}) t^{l_1 l_2}_{l_3 l_4}, \quad \text{(D5)}$$

where we drop the label L from the extra-reduced trispectrum. The extra-reduced trispectrum now has the following mode expansion:

$$t^{l_1 l_2}_{l_3 l_4} = N \Delta_\Phi^3 \sum_m \alpha^{\mathcal{Q}}_m \int dr r^2 \mathcal{Q}^{l_1 l_2 l_3 l_4}_m(r), \quad \text{(D6)}$$

where now we have

$$\mathcal{Q}^{l_1 l_2 l_3 l_4}_m(r) = q^{l_1}_p(r) q^{l_2}_r(r) q^{l_3}_s(r) q^{l_4}_u(r) \quad \text{(D7)}$$

with

$$q^l_p(r) = \frac{2}{\pi} \int dk q_p(k) \Delta_l(k) j_l(kr). \quad \text{(D8)}$$

The mode decomposition is similar to that described in Sec. V with r_v = constant. In this case we use the following primordial decomposition:

$$(k_1 k_2 k_3 k_4)^2 \mathcal{T}_{\Phi,0}(k_1, k_2, k_3, k_4) = \sum_m \alpha^{\mathcal{Q}}_m q_p(k_1) q_r(k_2) q_s(k_3) q_t(k_4). \quad \text{(D9)}$$

Using this in the expression for the general estimator (32), which can be reexpressed as

$$\mathcal{E} = \frac{12}{N_T}\sum_{l_i m_i}\mathcal{T}_{l_1 m_1 l_2 m_2 l_3 m_3 l_4 m_4}(a_{l_1 m_1} a_{l_2 m_2} a_{l_3 m_3} a_{l_4 m_4})^{\rm obs}_c \tag{D10}$$

with

$$\begin{aligned}(a_{l_1 m_1} a_{l_2 m_2} a_{l_3 m_3} a_{l_4 m_4})^{\rm obs}_c = {} & a^{\rm obs}_{l_1 m_1} a^{\rm obs}_{l_2 m_2} a^{\rm obs}_{l_3 m_3} a^{\rm obs}_{l_4 m_4} - ((-1)^{m_1} C_{l_1}\delta_{l_1 l_2}\delta_{m_1 - m_2} a^{\rm obs}_{l_3 m_3} a^{\rm obs}_{l_4 m_4} + 5 \text{ perms}) \\ & + ((-1)^{m_1+m_3}\delta_{l_1 l_2}\delta_{m_1 - m_2}\delta_{l_3 l_4}\delta_{m_3 - m_4} C_{l_1} C_{l_3} + 2 \text{ perms}),\end{aligned} \tag{D11}$$

we find

$$\begin{aligned}\mathcal{E} = {} & \frac{12 N \Delta^3_\Phi}{N_T}\sum_m \alpha^{\mathcal{Q}}_m \int d\hat{n}\int dr r^2 [M_p(\hat{n}, r) M_r(\hat{n}, r) M_s(\hat{n}, r) M_t(\hat{n}, r) - (M^{\rm uc}_{pr}(\hat{n}, r) M_s(\hat{n}, r) M_t(\hat{n}, r) + 5 \text{ perms}) \\ & + (M^{\rm uc}_{pr}(\hat{n}, r) M^{\rm uc}_{st}(\hat{n}, r) + 2 \text{ perms})],\end{aligned} \tag{D12}$$

where

$$M_p(\hat{n}, r) = \sum_{lm}\frac{a_{lm} Y_{lm}(\hat{n})}{C_l} q^l_p(r), \qquad M^{\rm uc}_{pr}(\hat{n}, r) = \sum_{lm}\frac{Y^*_{lm}(\hat{n}) Y_{lm}(\hat{n})}{C_l} q^l_p(r) q^l_r(r). \tag{D13}$$

We again can estimate the computational time needed to find this estimator. Since we now have only one line of sight integral and one integral over the sky $\sim \int d\hat{n}$, we use the prescription outline in Sec. VI to estimate the complexity conservatively as $\mathcal{O}(100) \times \mathcal{O}(l^3_{\rm max})$.

The implementation in the case of the late-time estimator for which the extra-reduced trispectrum is independent of L can be found similarly. Since this estimator no longer requires a line of sight integral, the complexity of the calculation can be estimated as $\mathcal{O}(l^3_{\rm max})$.

[1] J. R. Fergusson, M. Liguori, and E. P. S. Shellard, arXiv:0912.5516 [Phys. Rev. D (to be published)].
[2] J. R. Fergusson and E. P. S. Shellard, Phys. Rev. D **76**, 083523 (2007).
[3] J. R. Fergusson and E. P. S. Shellard, Phys. Rev. D **80**, 043510 (2009).
[4] X. Chen, arXiv:1002.1416.
[5] P. Adshead, R. Easther, and E. A. Lim, Phys. Rev. D **80**, 083521 (2009).
[6] N. Bartolo, E. Dimastrogiovanni, S. Matarrese, and A. Riotto, J. Cosmol. Astropart. Phys. 11 (2009) 028.
[7] Q-G. Huang, J. Cosmol. Astropart. Phys. 06 (2009) 035.
[8] J.-L. Lehners and S. Renaux-Petel, Phys. Rev. D **80**, 063503 (2009).
[9] Y. Rodríguez and C. A. Valenzuela-Toledo, Phys. Rev. D **81**, 023531 (2010).
[10] D. Seery and J. E. Lidsey, J. Cosmol. Astropart. Phys. 01 (2007) 008.
[11] D. Seery, J. E. Lidsey, and M. S. Sloth, J. Cosmol. Astropart. Phys. 01 (2007) 027.
[12] D. Seery, M. S. Sloth, and F. Vernizzi, J. Cosmol. Astropart. Phys. 03 (2009) 018.
[13] C. A. Valenzuela-Toledo and Y. Rodríguez, Phys. Lett. B **685**, 120 (2010).
[14] X. Chen, B. Hu, M-x. Huang, G. Shiu, and Y. Wang, J. Cosmol. Astropart. Phys. 08 (2009) 008.
[15] F. Arroja, S. Mizuno, K. Koyama, and T. Tanaka, Phys. Rev. D **80**, 043527 (2009).
[16] X. Chen, M-x. Huang, and G. Shiu, Phys. Rev. D **74**, 121301 (2006).
[17] F. Arroja and K. Koyama, Phys. Rev. D **77**, 083517 (2008).
[18] S. Mizuno, F. Arroja, and K. Koyama, Phys. Rev. D **80**, 083517 (2009).
[19] L. Senatore and M. Zaldarriaga, arXiv:1004.1201.
[20] X. Gao and B. Hu, J. Cosmol. Astropart. Phys. 08 (2009) 012.
[21] Q-G. Huang, arXiv:1004.0808.
[22] K. Izumi and S. Mukohyama, J. Cosmol. Astropart. Phys. 06 (2010) 016.
[23] X. Chen and Y. Wang, J. Cosmol. Astropart. Phys. 04 (2010) 027.
[24] S. Renaux-Petel, J. Cosmol. Astropart. Phys. 10 (2009) 012.
[25] M. Sasaki, J. Väliviita, and D. Wands, Phys. Rev. D **74**, 103003 (2006).
[26] M. Hindmarsh, C. Ringeval, and T. Suyama, Phys. Rev. D **80**, 083501 (2009).
[27] D. M. Regan and E. P. S. Shellard, arXiv:0911.2491.
[28] E. Sefusatti, Phys. Rev. D **80**, 123002 (2009).
[29] P. Vielva and J. L. Sanz, arXiv:0910.3196.
[30] L. Alabidi and D. Lyth, J. Cosmol. Astropart. Phys. 05 (2006) 016.
[31] J. Smidt, A. Amblard, C. T. Byrnes, A. Cooray, and D. Munshi, Phys. Rev. D **81**, 123007 (2010).
[32] J. Smidt, A. Amblard, A. Cooray, A. Heavens, D. Munshi,

and P. Serra, arXiv:1001.5026.
[33] N. Kogo and E. Komatsu, Phys. Rev. D **73**, 083007 (2006).
[34] W. Hu, Phys. Rev. D **64**, 083005 (2001).
[35] R. Scoccimarro, E. Sefusatti, and M. Zaldarriaga, Phys. Rev. D **69**, 103513 (2004).
[36] M. Liguori, E. Sefusatti, J. R. Fergusson, and E. P. S. Shellard, arXiv:1001.4707.
[37] L. Amendola, Mon. Not. R. Astron. Soc. **283** 983 (1996).
[38] D. Babich, Phys. Rev. D **72**, 043003 (2005).
[39] E. Komatsu, Classical Quantum Gravity **27**, 124010 (2010).
[40] D. M. Regan, J. R. Fergusson, E. P. S. Shellard, and M. Liguori (unpublished).
[41] C. T. Byrnes, M. Sasaki, and D. Wands, Phys. Rev. D **74**, 123519 (2006).
[42] K. M. Smith and M. Zaldarriaga, arXiv:0612571.
[43] T. Okamoto and W. Hu Phys. Rev. D **66**, 063008 (2002).